Master Thesis

Expression, purification, and interaction studies between TRIM25 E3 ubiquitin ligase and Dicer endonuclease

Lauri Vuorenpää

University of Jyväskylä

Department of Biological and Environmental Science

Cell- and Molecular Biology

25.04.2023

Dicer endonuclease and TRIM25 E3 ubiquitin ligase are key players in an innate immune antiviral response. TRIM25 can activate RIG-I signaling pathway, which leads to production of type 1 interferons. TRIM25 recognizes and binds to substrates via its CC- and PRYSPRY domains. Small non-coding RNAs, microRNAs (miRNAs) and small-interfering RNAs (siRNAs) are important gene regulators that work post-transcriptionally. Dicer is involved in a miRNA and siRNA pathways where it processes precursor RNAs into small RNAs.

Previous studies have showed, that the TRIM25 can interact with Dicer´s helicase domain (Hel2i2) via its PRYSPRY domain, but the interaction has not been characterized on a residue level yet. In this thesis, Dicer Hel2i2, TRIM25 PRYSPRY and TRIM25 CC-PRYSPRY were recombinantly expressed and purified and the interaction between TRIM25 and Dicer were characterized with structural biology methods. We were able to set working expression and purification protocol for the Dicer Hel2i2 domain and get more insight for its biochemical properties. Interaction studies with Dicer and TRIM25 were not sufficient to detect binding between the proteins.

Dicer endonukleaasilla ja TRIM25 E3 ligaasilla on merkittävä rooli synnynnäisen immuniteetin antiviraalissa vasteessa. TRIM25 aktivoi RIG-I signalointireittiä, joka johtaa tyypin 1 interferonien tuotantoon. TRIM25 tunnistaa ja sitoutuu substraatteihinsa sen CC- ja PRYSPRY-domeenien avulla. Pienet ei-koodaavat RNA:t, kuten mikroRNAt (miRNAt) ja pienet häiritsevät RNA:t (siRNAt) ovat tärkeitä post-transkriptionallisesti toimivia geenin säätelijöitä. Dicer vaikuttaa miRNA ja siRNA molekyylien tuotantoon pilkkomalla niiden esiasteita lyhyiksi RNA:ksi.

Aikaisemmat tutkimukset ovat osoittaneet, että TRIM25 voi vuorovaikuttaa Dicer helikaasi-domeenin (Hel2i2) kanssa sen PRYSPRY- ja CC-domeenien avulla, mutta vuorovaikutusta ei olla aikaisemmin karakterisoitu. Tässä tutkimuksessa, tuotimme rekombinanttisesti Dicer Hel2i2, TRIM25 PRYSPRY ja TRIM25 CC-PRYSPRY domeenit ja Dicerin ja TRIM25:n välistä vuorovaikutusta tutkittiin rakennebiologisin menetelmin. Onnistuimme luomaan Dicer Hel2i2:lle toimivan ekspressio- ja puhdistusprotokollan ja saimme lisää tietoa sen biokemiallista ominaisuuksista. Tutkimuksemme ei tuottanut tarpeeksi dataa, jotta Dicerin ja TRIM25 välistä vuorovaikutusta olisi saatu kartoitettua.

TABLE OF CONTENTS

GLOSSARY AND ABBREVIATIONS

GLOSSARY

Cytoplasmic receptor   Molecules found in the cytoplasm that bind to substrate and causes specific effect in the cell.

E3 Ubiquitin ligase   Protein that acts in a final step of three-enzyme ubiquitin transfer cascade.

Endorinuclease   Enzyme which cleaves RNA.

Interferon   Belong to family of cytokines and has antiviral properties. Produced and released from cells by immune system response to pathogens or cytokines.

ABBREVIATIONS

AGO   argonaute protein

CARD   caspase recruitment protein

dsRNA   double-stranded RNA

dsRBD   double-stranded RNA Binding Domain

MAVS   mitochondrial antiviral signalling protein

RIG-I   retinoic acid-inducible gene-I

RLR   RIG-I-like receptor

TRIM   tripartite motif

1 INTRODUCTION

Innate immunity has diverse mechanisms to protect us from viral threads (Maillard et al. 2019). It consists of sensors that can recognize pathogen-associated molecular patterns (PAMPs) and effectors which dispose pathogens (Ahmad & Hur, 2015). Helicases are ubiquitous and commonly known for their ability to unwind nucleic acid double helices, but they can also contribute to innate immunity by working as a sensors or effectors (Ahmad & Hur, 2015).

RNA Helicases, which bind or remodel RNA or RNA-protein complexes, can be classified to superfamilies according to their sequence and structural features (Linder & Jankowsky 2011, Fairman-Williams et al., 2010). Most of the RNA helicases belong to Superfamily 2 (SF2) (Jankowsky & Fairman, 2007). RIG-I like proteins (RLRs: RIG-I like receptors) are one of five different sub-families in SF2 superfamily and they work as a cytoplasmic receptor for PAMPs (Leitão et al. 2015).

RNA interference (RNAi) and the interferon system (IFN) are both antiviral mechanisms triggered by viral RNA (Leitão et al. 2015, Maillard et al. 2019). However, mammalian cells rely more on the IFN system and plants, insects, nematodes, and fungi rely on RNAi for natural antiviral defense (Li et al. 2013, Maillard et al. 2019, Schuster et al. 2019). The IFN system launches, when RLRs detect viral RNA and trigger production of type I interferons (IFN) (Maillard et al. 2019). IFNs will then activate interferon-stimulated genes (ISGs) that encode proteins with antiviral properties (Maillard et al. 2019). In antiviral RNAi, the Dicer enzyme cleave virus-derived double stranded RNA (dsRNA) into small interfering RNAs (siRNAs) and unwound the duplex RNA (Song et al. 2017). RNA-induced silencing complex (RISC) is formed from one of the RNA strands, AGO, Dicer and other additional accessory proteins (Luo et al. 2012, Song et al. 2017). RISC complex then recognize viral RNA by complementary base pairing with the help of the

single-stranded RNA molecule and can guide the degradation or suppress the translation of viral RNA (Song et al. 2017).

1. RIG-I SIGNALING PATHWAY AND TRIM25

RIG-I signaling pathway triggers the production of IFNs. Retinoic-acid-inducible gene-1 (RIG-I), undergoes a conformational change upon recognition of viral RNA (D´Cruz et al. 2013). This will lead to RIG-I CARD domain to interact with mitochondrial antiviral signaling protein (MAVS) on the mitochondrial outer membrane (Nguyen et al. 2016). Activated MAVS triggers phosphorylation-mediated dimerization of the transcription factors IRF3/7 and NF-kB to express type 1 interferons. (Heikel et al. 2016, Choudhury et al. 2017, Nguyen et al. 2016).

RIG-I mediated signaling pathway is regulated by ubiquitination (Nguyen et al. 2016). Ubiquitination is a versatile post-translational modification that can target proteins for degradation or regulate their activation (Zheng et al. 2017). Ubiquitin is covalently attached to target protein by three-step enzymatic cascade, what consists of three classes of enzymes; E1 (activation), E2 (conjugation) and E3 (ligation) (Shaid et al. 2013). Small 76-residue ubiquitin contains seven lysines (K6, K11, K27, K29, K33, K48 and K63), which can be conjugated to another ubiquitin molecule to form different types of polyubiquitin chains (Akutsu 2016). One of the regulators is tripartite motif containing protein 25 (TRIM25), an E3 ubiquitin ligase mediating RIG-I activation by inducing K63 poly-ubiquitination on one of the two CARD domains of RIG-I (Williams et al. 2019).

Originally identified in estrogen-responsive gene, TRIM25 has multiple functions in innate immunity, morphogenesis, and cell proliferation (D´Cruz et al. 2013, Williams et al. 2019). Like most of the TRIM proteins, TRIM25 has an N-terminal RBCC motif, which consists of RING, two B-boxes and Coiled-Coil (CC) domains (Williams et al. 2019). CC domain is responsible for TRIM25 dimerization and

oligomerization (Choudhury et al. 2017). In C-terminal TRIM25 has a PRYSPRY domain which is connected to the CC domain with a 73-residue long linker (L2) (Koliopoulos et al. 2018).
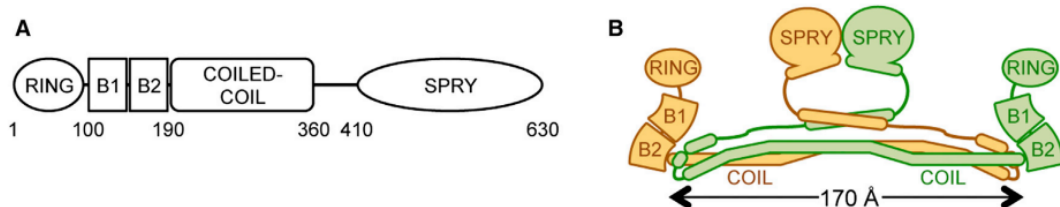
Figure 1 (A) Schematic structure of TRIM25 E3 Ligase domain organization. (B) Schematic structure of TRIM25 antiparallel dimer (Sanchez et al. 2016).

1.1 TRIM25 PRYSPRY DOMAIN

PRYSPRY domain (22 kDa, 192 residues) consists of 60 amino acid PRY segment (residues 439-512) and 140 residues SPRY (residues 513-633) regions (Kowalinski 2010). It has an immunoglobulin-like fold and hydrophobic core with total of thirteen β-strands (D´Cruz et al. 2013, Kowalinski 2010). These β-strands forms two antiparallel β-sheets in a bent β-sandwich configuration (D´Cruz et al. 2013). In the N-terminus there are also two a-helices with α1 almost parallel and α2 perpendicular to the direction of the β-strands (D´Cruz et al. 2013, Kowalinski 2010). Overview of the structure of PRYSPRY are shown in Figure 2. Even though the core is highly conserved, PRYSPRY has six flexible regions (V1-6) which allows binding to broad variety of substrates, such as linear peptide epitopes and multi-protein assemblies including antibodies and viral capsids (Vaishali et al. 2021, Williams et al. 2019). How PRYSPRY domains recognize substrates and regulates immune

function is still unclear (Kato et al. 2021). The domain is also responsible for binding TRIM25 to RNA (Choudhury et al. 2017). Viral antigens, such as SARS-CoV nucleocapsid protein, can also inhibit TRIM25 activity by binding to PRYSPRY domain (Choudhury et al. 2017).
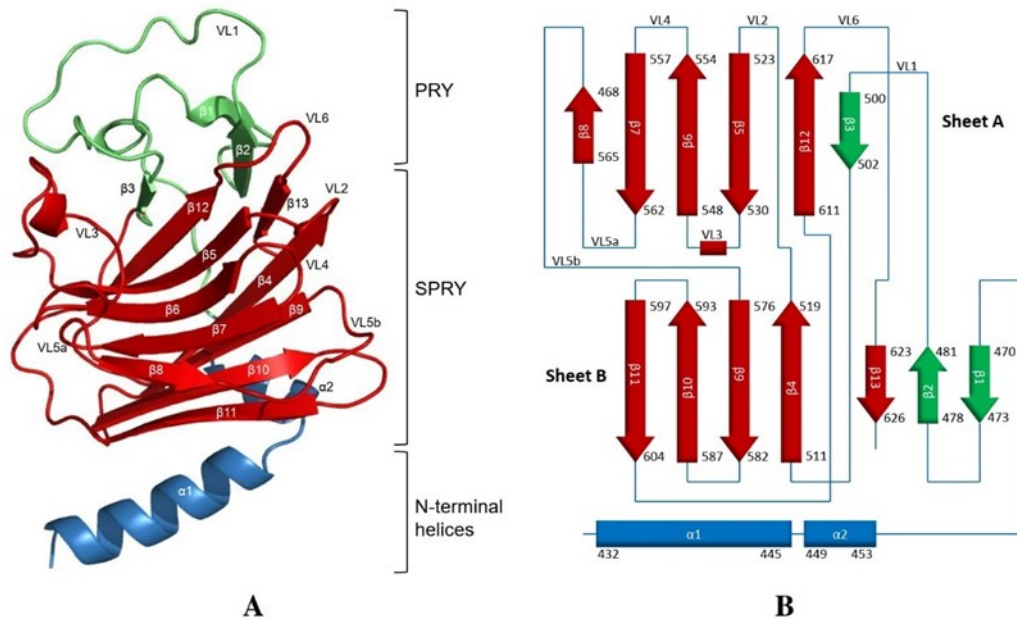
Eva Kowalinski. Structural studies of host-virus interactions looking at two examples: the innate immunity receptor RIG-I and the influenza virus RNA polymerase endonuclease.
Biochemistry, Molecular Biology. Université Joseph-Fourier - Grenoble I, 2010. English. tel-00752678

Figure 2 Structure of TRIM25 PRYSPRY. Sheet A is formed from β-strands 3, 12, 5, 6, 7 and 8. Sheet B is formed from strands 1, 2, 13, 4, 9, 10 and 11. Helices a1 and a2 are found outside of the β-sandwich to sheet B, Variable loop regions (VL1-6) marked in figure (Kowalinski 2010).

1.2 DICER

Dicer endonuclease is a class IV RNase III enzyme and found in many eukaryotic organisms (Song et al. 2017). It specifically hydrolyzes phosphodiester bonds found

in dsRNA, ending up generating short RNAs, which makes it in major role in the biogenesis of small regulatory RNAs (Ciechanowska et al. 2021, Paturi et al. 2020).

As a 218-kDa multidomain, human Dicer consist of helicase domain, a DUF283 domain, a dsRNA-binding domain (dsRBD), a PAZ domain and two RNase III domains (Korhonen et al. 2011, Figure 3, Table 1). The domains are homologous across the eukaryotes, but many species have more than one Dicer with different domain architecture for functional advantages (Paturi, 2021).

Paturi S and Deshmukh MV (2021) A Glimpse of "Dicer Biology" Through the Structural and Functional Perspective. Front. Mol. Biosci. 8:643657. doi: 10.3389/fmolb.2021.643657
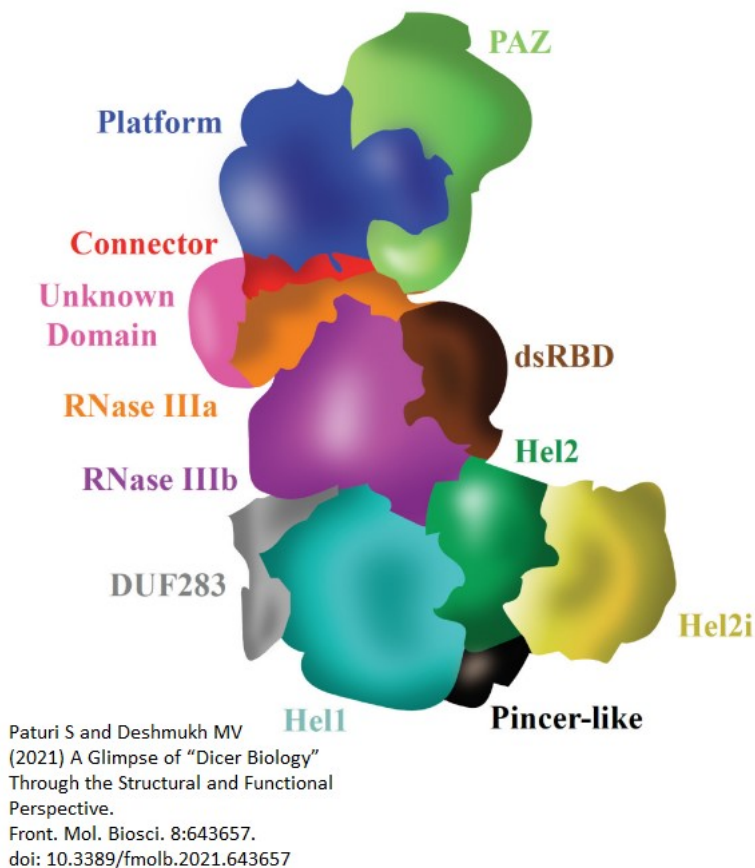
Figure 3 Structure of Dicer (Paturi & Deshmukh, 2021).

1.3 DICER HELICASE DOMAIN

Dicer's helicase domain belongs to RIG-I Like Receptor (RLR) proteins due to its similarity to RIG-I-like receptors (Hansen et al. 2019, Kato et al. 2021). The helicase domain has ability to bind dsRNA (Kato et al.2021) and human Dicer is auto-inhibated by the helicase domain (Ma et al., 2008). Cleavage of long dsRNA is done by Dicer helicase domain (Song et al. 2017).

Crystal structure of the human Dicer helicase has not been characterized yet, but the structure has been predicted by using cryo-EM models and other biochemical studies (Svobodova et al. 2015). Helicase domain sits on the bottom part of the L-shaped human Dicer (Paturi, 2021). It consists of three globular subdomains Hel1, Hel2 and Hel2i and they form a C-shaped structure (Liu et al. 2018). Hel1 is located in the junction of the L and interacts with DUF283 and RNase IIIb domains (Liu et al. 2018). Hel2 is located in the center of the helicase domain and Hel2i is at the very end of the short arm of Dicer (Liu et al. 2018). Hel2 and Hel1 has a four or five β-strands surrounded by several α-helices and the subdomains are connected by α-helix called pincer-like motif (Liu et al. 2018). Flexible pincer-like motif allows the Hel2 and Hel2i domains to have various orientations around the Hel1 domain (Liu et al. 2018). The Hel2i domain is characterized by four antiparallel α-helices (Liu et al. 2018). Hel1 can unwind RNA and DNA duplexes (Ciechanowska et al. 2021)
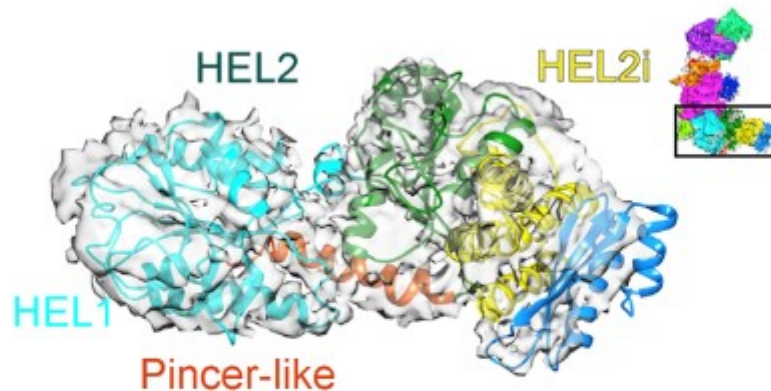
Figure 4 Structure of human Dicer Helicase domain atomic model fitted in to cryo-EM density according to Liu et al. 2018.

1.4 AIM OF THE THESIS

Recent discovery of the relationship between RNA helicases and TRIM ubiquitin ligases has revealed that the TRIM proteins interact with RIG-I-like receptors through their PRYSPRY domain (Kato et al. 2021). PRYSPRY domain binds to two adjacent α-helices in the Hel2 subdomain, α1 and α3 (Kato et al. 2021). Variable loop regions (VL), especially VL1, VL3 and VL6 has been shown to be in important role in the binding surface of the PRYSPRY domain towards the helicases (Kato et al. 2021). L1 and L2 linker residues of Dicer Hel2 which are equivalent to α3 and α1 helicases of RLRs are important for Hel2 binding (Kato et al. 2021).

Even though the engagement of the TRIM25 PRYSPRY and Dicer Hel2 domains has been revealed, the interactions has not been characterized before on a residue level. The primary aim of this thesis is to characterize the interaction between TRIM25 PRYSPRY domain and Dicer Helicase domain via structural biology methods. These

methods include NMR spectroscopy, SEC-MALS and mass photometry. As Kato et al. proposed, the interaction with TRIM25 and helicase enzymes is avidity dependent, we will also use TRIM25 CC-PRYSPRY construct, due to its native dimeric state. In Kato´s research, the isolated Hel2 was insoluble and required inclusion of the domain Hel2i. We will include both subdomains Hel2 and Hel2i in our protein construct, referred as Hel2i2 domain. In this study. we perform binding experiments with Dicer Hel2i2, TRIM25 PRYSPRY and TRIM25 CC-PRYSPRY domain constructs. The hypothesis is that Dicer Hel2i2 interacts with TRIM25 CC-PRYSPRY but not with TRIM25 PRYSPRY due to CC-PRYSPRY domains native dimeric structure. The interaction surface is believed to be L1 and L2 linker residues of Dicer Hel2 and VL regions of PRYSPRY domain.

To study these interactions, the proteins must be first expressed and purified. Secondary aim of the study is to set working expression and purification protocol for the Dicer Hel2i2 domain. For TRIM25 PRYSPRY and TRIM25 CC-PRYSPRY we already have a working expression and purification protocol.

Biological functions and mechanisms of Dicer and TRIM25 is still poorly understood, and our findings might provide new insight of the interaction between these proteins. Also, our findings might help us to understand more the role of human Dicer and TRIM25 in antiviral response.

2. MATERIALS AND METHODS

2.1 Transformation of Dicer Hel2i2 and TRIM25 CC-PRYSPRY

We used the same transformation protocol to the domains of Dicer Hel2i2 and TRIM25 CC-PRYSPRY. For Dicer Hel2i2 we used ampicillin containing LB agar plates and for the TRIM25 CC-PRYSPRY we used kanamycin, chloramphenicol and spectinomycin resistant LB agar plates. 50 ng of DNA was pipetted to BL21(DE3)

competent cells in a transformation tube. The mixture was incubated on ice for 30 minutes. 30 second heat shock at 42 °C was applied to the mixture and put back on ice for 2 min after the heat shock. 100 µl of SOC media was added and incubated in a shaking incubator for 60 min at 37 °C and 900 rpm. After the incubation the mixture was centrifuged 12000 rpm for 2 minutes. Small amount of suspension was discarded, and the pellet was resuspended. The transformed cells were plated to appropriate antibiotic containing 10 cm LB agar plates and incubated at 37 °C overnight.
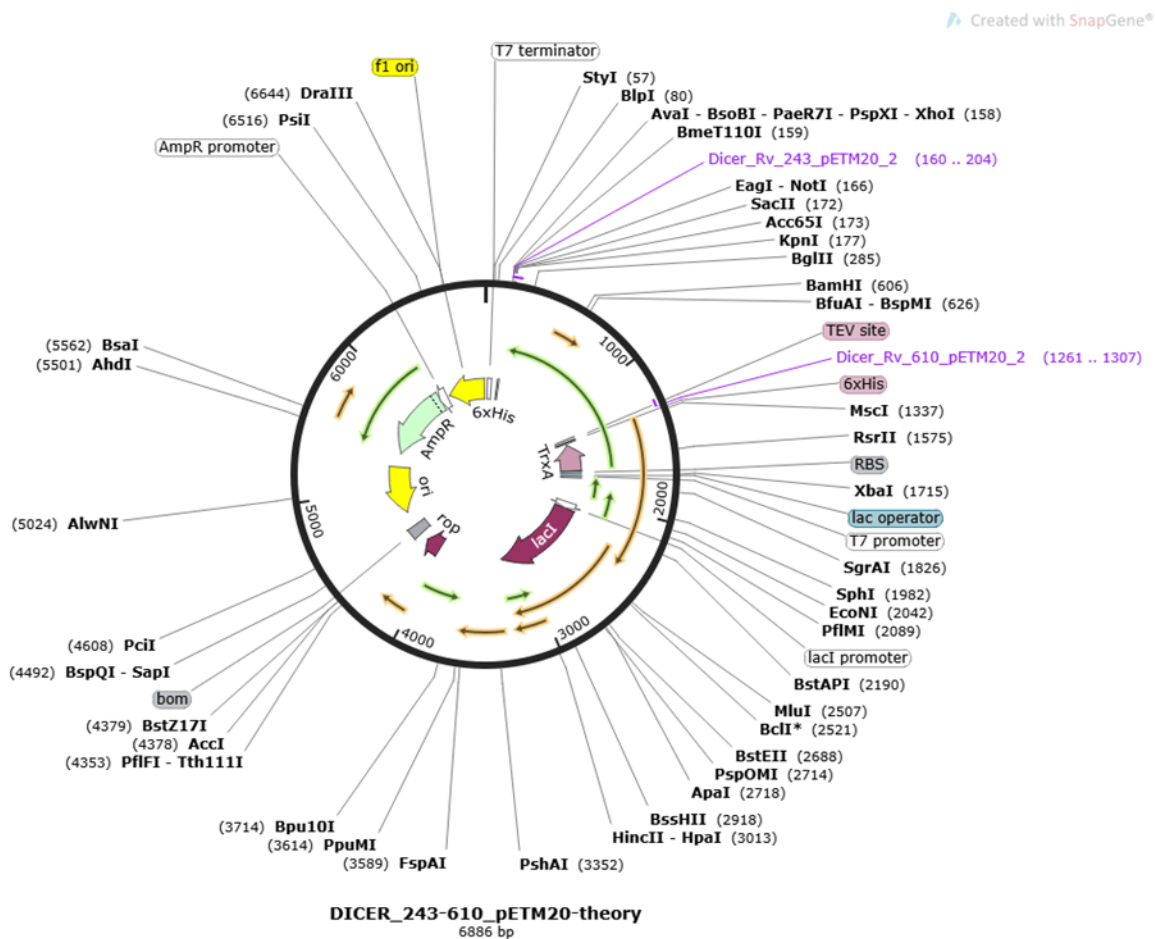

Figure 5 Plasmid used in Dicer Hel2i2 transformation.

2.2 Protein expression and purification

All the purification steps were done with the NGC chromatography system (Bio-Rad). For 15N isotope labeling, proteins were expressed in M9 medium with 15N NH$_4$Cl (0.5 g/l) as nitrogen source. The success of each purification step was monitored by running a sodium dodecyl sulfate-polyacrylamide gel electrophoresis (SDS-PAGE) after each purification step.

2.2.1 Purification of Dicer Hel2i2 domain

Dicer Hel2i2 domain corresponding to residues 243-610 was cloned to pETm20 ampicillin resistant expression vector (EMBL, Germany). The protein construct carried an N-terminal polyhistidine affinity tag domain (His-Tag).

Dicer Hel2i2 was expressed in BL21(DE3) strand E. coli cells and grown in Lysogeny Broth (LB) medium with 0,1 M ampicillin.

Cell culture was incubated at 37 °C in the shaker (Kühner ISF-1-W). The temperature was lowered to 18 °C when the OD of the cell culture was at 0.4. Protein production of the Dicer Hel2i2 domain was induced with 2 mM IPTG when OD of the cell culture was 0.6. The cells were further incubated at 17 °C for 20 hours. Cells were centrifuged at 16,000 rpm for 20 min at 4 °C to clear the lysate. Pellet was resuspended in a lysis buffer (50 mM Tris:Cl pH 7.5, 0.3 M NaCl, 10mM Imidazole, 10 mM B-ME) and put in the freezer for 1 hour. Tablet of protease-inhibitor (c0mplete, Roche), lysozyme (1 mg/ml) and benzonase (0.8 ul/ml) was added to lysate and incubated 40 min at room temperature. The cells were lysed by using the microfluidizer and then centrifuged at 18,000 rpm for 30 min at 4 °C (Beckman Coulter Allegra 64R). Lysate was filtered with Millex® HV 0.45 µm filter (Merck Millipore).

Proteins were first purified by using Immobilized Metal Affinity Chromatography (IMAC) with 5 ml HisTrap HP column and IMAC buffer (50 mM Tris:Cl pH 7.5, 0.3

M NaCl, 10 mM Imidazole). Imidazole was used to elute Dicer Hel2i2 domain. Fractions containing protein was pooled and then dialysed overnight at 4 °C with dialysis buffer (50 mM Tris:Cl pH 7.5, 0.3 M NaCl, 10 mM Imidazole) and cleavage was done with His-Tev (Tobacco Etch Virus) protease.

His-Tag and Dicer Hel2i2 domain were separated by using a 5 ml HisTrap HP column. Cleaved Dicer Hel2i2 domain doesn't interact with the column, so flowthrough from the outlet valves was collected. Protein was further dialysed with 20 mM Sodium phosphate pH 6.5, 500 mM NaCl, 0.2 mM TCEP, 5 % Glycerol. Next, the protein was concentrated to a final volume of 1 ml and centrifuged at 12 min 16100 rpm, at 4 °C to remove aggregations. Concentration was measured using a Nanodrop ND-1000 spectrophotometer (Peqlab).

Sample was further purified with the Superdex S75 10/300 size exclusion column with buffer 20 mM Sodium phosphate pH 6.5, 150 mM NaCl, 0.2 mM TCEP. Fractions containing Dicer Hel2i2 were pooled and concentrated with Amicon® Ultra-15 concentrator (10 kDa MWCO, Merck Millipore) to the final concentration of 10 mg/ml and centrifuged at 12 min 16100 rpm, at 4 °C to remove aggregations. All the purification steps were done with the NGC chromatography system (Bio-Rad). The concentration of samples was measured with Nanodop ND-1000 (Peqlab) spectrophotometer.

2.2.2 Purification of TRIM25 PRYSPRY domain and TRIM25 CC-PRYSPRY domain

For the TRIM25 PRYSPRY domain (PDB: 6FLM) corresponding to residues 439 to 630 and TRIM25 CC-PRYSPRY domain (corresponding to residues 189-630, PDB: 6FLN) we used the same expression and purification protocol from Haubrich et al. 2020.

Both domains were expressed in pETm22 kanamycin resistant and coexpressed with the plasmids of the chaperones KJE, ClpB and GroELS (Chloramphenicol and

Spectinomycin resistant). Chaperones assists the folding of PRYSPRY domain to the native state and prevents its aggregation (de Marco et al. 2007). ^{15}N-M9 media was used for labeled samples and LB media was used for unlabeled samples.

Cell culture was incubated at 37 °C in the shaker (Kühner ISF-1-W). The temperature was lowered to 18 °C when the OD of the cell culture was at 0.4. Protein production of the domains was induced with 2 mM Isopropyl β-D-1-Thiogalactopyranoside (IPTG) when OD600 of the cell culture was 0.6. The cells were further incubated at 17 °C for 20 hours. Cells were centrifuged at 16,000 rpm for 20 min at 4 °C. Pellets were resuspended in a lysis buffer (50 mM Tris:Cl pH 7.5, 0.3 M NaCl, 10mM Imidazole, 10 mM B-ME) and put in the freezer for 1 hour. Tablet of protease-inhibitor (c0mplete, Roche), lysozyme (1 mg/ml) and benzonase (0.8 ul/ml) was added to lysate and incubated 40 min at room temperature. The cells were lysed by using the microfluidizer and then centrifuged at 18,000 rpm for 30 min at 4 °C (Beckman Coulter Allegra 64R). Lysate was filtered with Millex® HV 0.45 µm filter (Merck Millipore).

Proteins were first purified by using Immobilized Metal Affinity Chromatography (IMAC) with 5 ml HisTrap HP column and IMAC buffer (50 mM Tris:Cl pH 7.5, 0.3 M NaCl, 10 mM Imidazole). After sample injection, ATP wash was done to remove chaperones (ATP buffer: 50 mM Tris pH 7.5, 350 mM KCl, 5 mM MgCl2, 1 mM ATP, injection volume 20 ml, incubation time 30 min.) Imidazole was used to elute TRIM25 PRYSPRY domain. Fractions containing protein was pooled and dialyzed overnight at 4 °C with dialysis buffer (20 mM BisTris pH 6.0, 100 mM NaCl, 5% Glycerol, 2 mM B-ME) and cleavage was done with His-3C protease.

Next, proteins were purified by cation exchange chromatography with HiTrap FF column and SP buffer (20 mM BisTris pH 6.0, 100 mM NaCl, 2 mM B-ME). Fractions containing protein were pooled and concentrated with Amicon® Ultra-15 concentrator (10 kDa MWCO, Merck Millipore) to the volume of 1 ml and centrifuged at 12 min 16100 rpm, at 4 °C to remove aggregations.

Protein was further purified by size exclusion chromatography (SEC) with a Superdex 200 column in SEC buffer (20 mM Sodium phosphate ph 6.5, 150 mM NaCl, 0.2 mM TCEP).

2.3 Thermal stability assay on Dicer Hel2i2

Thermal shift assay was performed to find stabilizing conditions for Dicer Hel2i2 with Nano differential scanning fluorimetry (NanoDsf). NanoDsf is a dye-free method to study thermal stability of proteins. It measures the intrinsic fluorescence intensity ratio of aromatic amino acid tryptophan as a function of temperature (Wen et al. 2020). Location of aromatic amino acid residues changes during protein unfold, which leads to changes in the fluorescence spectra (Wen et al. 2020). Based on this principle, the NanoDsf determines the thermal transition (unfold) temperature (T_m) and onset temperature (T_{onset}) by measuring the ratio of the fluorescence intensity at 330 nm and 350 nm as a function of temperature (Kim et al. 2021). Higher thermal transition temperature indicates more stable protein.

NanoDsf assays were carried out with Prometheus NT.48 (NanoTemper Technologies). The tested conditions varied with differences in salt concentration, protein concentration, pH and glycerol. Sample volume was 50 µl with the concentration of 23.38 µM (1 mg/ml) of protein. Samples were loaded in NanoDsf grade standard capillaries (NanoTemper Technologies). The temperature was increased by 1 °C per minute from 20 °C to 95 °C. The data was processed with PR.ThermControl software (NanoTemper Technologies).

2.4 Size Exclusion Chromatography - Multi Angle Light Scattering (SEC-MALS)

SEC-MALS assay was carried out to test if Dicer Helicase forms complexes with TRIM25 PRYSPRY or TRIM25 CC-PRYSPRY. We also wanted to see if the purification of Dicer Helicase domain was successful, and it acts as a monomer in a buffer used. Measurements were done on 1260 Infinity LC HPLC system (Agilent)

with MiniDawn scattering detector (Wyatt) and Optilab dRI detector (Wyatt). Superdex 200 10/300 GL column was used with the flowrate of 0.5 ml per minute. In all experiments we used as a buffer 20 mM Sodium phosphate pH 6.5, 150 mM NaCl, 0.2 mM TCEP. Data was analyzed and processed with ASTRA (7.3.1.9) software (WYATT technology). Theoretical weights of the proteins are: Dicer Hel2i2 = 42.8 kDa, TRIM25 PRYSPRY = 22.0 kDa and TRIM25 CC-PRYSPRY = 50.0 kDa.

First, Dicer Hel2i2 was ran in SEC-MALS in two different concentrations, 23.4 µM and 11.69 µM. We used two different concentrations to see if the concentration affects on Dicer Hel2i2 polymerization.

Dicer Hel2i2 and TRIM25 PRYSPRY, and TRIM25 CC-PRYSPRY was then ran in SEC-MALS each protein separately with 110 µl of sample volume and in concentration of 1 mg/ml. Then TRIM25 PRYSPRY-, and CC-PRYSPRY was ran in SEC-MALS with presence of Dicer Hel2i2 to see if they form a complex.

2.5 Mass Photometry assay

For molecular mass measurements we used Refeyn TwoMP mass photometer (Refeyn Ltd.). Mass photometry is a relatively new method to analyze molecules. It is label-free, and it measures mass at the single molecule level in a solution. When molecule encounters the measurement surface, the light scattered from the molecule interferes with the light reflected by measurement surface (Li et al. 2020). The signal of interference scales linearly with the mass of molecule (Li et al. 2020). We measured the mass of Dicer Hel2i2, TRIM25 PRYSPRY and TRIM25 CC-PRYSPRY individually and in the mixtures of Hel2i2 + PRYSPRY and Hel2i2 + CC-PRYSPRY. Refeyn TwoMP mass photometry mass range is from 30 kDa to 5 MDa, so we could not detect TRIM25 PRYSPRY monomer (22kDa).

All samples were measured in buffer 20 mM Sodium phosphate pH 6.5, 150 mM NaCl, 0.2 mM TCEP. Acquisition time was 1 minute with sample volume of 20 µl

and concentration of 10-50 nM. Acquired data were processed and analyzed with Discover MP v2.4.2 (Refeyn Ltd.).

2.6.1 NMR Titrations

All the NMR experiments were carried out using Bruker Avance III (700 MHz) spectrometer equipped with a room temperature triple resonance probe head. All the experiments were performed in 20 mM Sodium Phosphate, pH 6.5, 500 mM NaCl, 2 mM TCEP, 10 % D2O and 0.02% Sodium Azide. Protein samples were loaded to 5 mm Shigemi NMR tubes. At each titration point, a 1H-15N-HSQC spectra was recorded. Samples were measured at concentrations ranging between 27 and 107 µM. Spectra were processed with TOPSPIN, NMRpipe software (Delaglio et al., 1995) and analyzed with SPARKY software (NMRFAM-SPARKY 1.470 powered by Sparky 3.190, Goddard, T. D. & Kneller, D. G.).

2.6.2 1D NMR experiments

Whether protein forms oligomerizes or not may depend on various circumstances like pH, temperature, and salt concentration (Anglister et al. 1993). In the NMR spectrometer, the surrounding condition of the protein differs. We wanted to see if the Dicer Hel2i2 forms oligomers in different concentrations in the NMR spectrometer.

Oligomeric state of the protein can be estimated with 1-1 Spin Echo experiment (Sklenar & Bax, 1987). To see if the concentration effects on oligomeric state of Dicer Hel2i2 in the NMR spectroscopy, we ran 1-1 Spin Echo experiment in two different Dicer Hel2i2 concentrations (88.6 µM and 30 µM). Exchangeable NH proton signals are near the H_2O frequency, so they get easily saturated. However, 1-1 Spin echo experiment is an effective method to suppress water molecules in a water-soluble compound and get a baseline distortion free spectrum. This method uses 1-1 hard pulse as a read pulse and a 1-1 refocusing pulse (Sklenar & Bax, 1987).
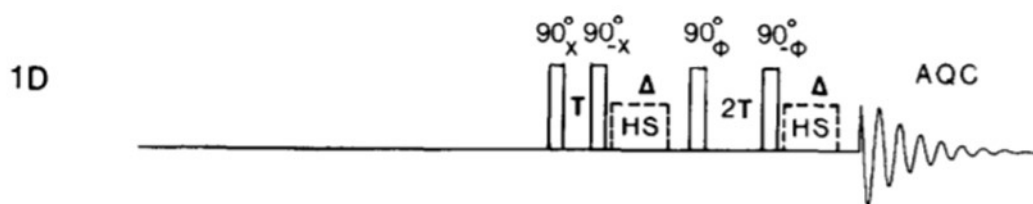
Sklenar, V. and Bax, A. (1987) J. Magn. Reson., 74, 469479.

Figure 6 1-1 echo scheme for 1D-spectra. Short homospoil (HS) pulses were applied during the delays to suppress water (Sklenar & Bax, 1987).

The rotational correlation (τ_c) time increases when proteins aggregate, and this results to increase of the resonance line width of the protons and heterenuclei. Average transverse relaxation time (T_2) of amide protons can be used when evaluating the approximate value of the rotational correlation time. τ_c (in ms) is approximately equal to $1/(T_2(\text{seconds}))$ (Anglister et al. 1993). Rotational correlation time of monomeric protein in solution in the temperature of 20°C is approximately 0.6 its molecular weight in kilodaltons (Anglister et al. 1993).

$$T_2 = \frac{\sim(-2)}{\ln(\frac{Ia}{Ib})},\tag{1}$$

$$\tau_c[ns] \approx \frac{1}{5 \, x \, T_2},\tag{2}$$

$$\tau_c \sim \frac{1}{2}MWT[kDa]\tag{3}$$

Acquired 1D NMR spectrum were overlaid to reference spectrum to get the ratio of I_A/I_B. Following formulas (1,2 and 3) was used to approximate the molecular weight of the NMR sample.

I_A/I_B is the ratio of sample and reference spectrum integrated value of signal on the ^{1}H spectrum.

3 RESULTS

3.1 Expression and purification of TRIM25 PRYSPRY and TRIM25 CC-PRYSPRY domains

With TRIM25 PRYSPRY domain we did not have any problems with the purification. Final concentrations of TRIM25 PRYSPRY were 1.09-5.54 mg/ml from 6 l expression yield.

Figure 7 SEC of TRIM25 PRYSPRY and SDS-PAGE gel corresponding to peaks. Green line of the chromatogram shows the UV of 280 nm.

We had troubles purifying the TRIM25 CC-PRYSPRY domain. Throughout the purification, there were degenerated bands on an SDS-PAGE gel (Figure 8).
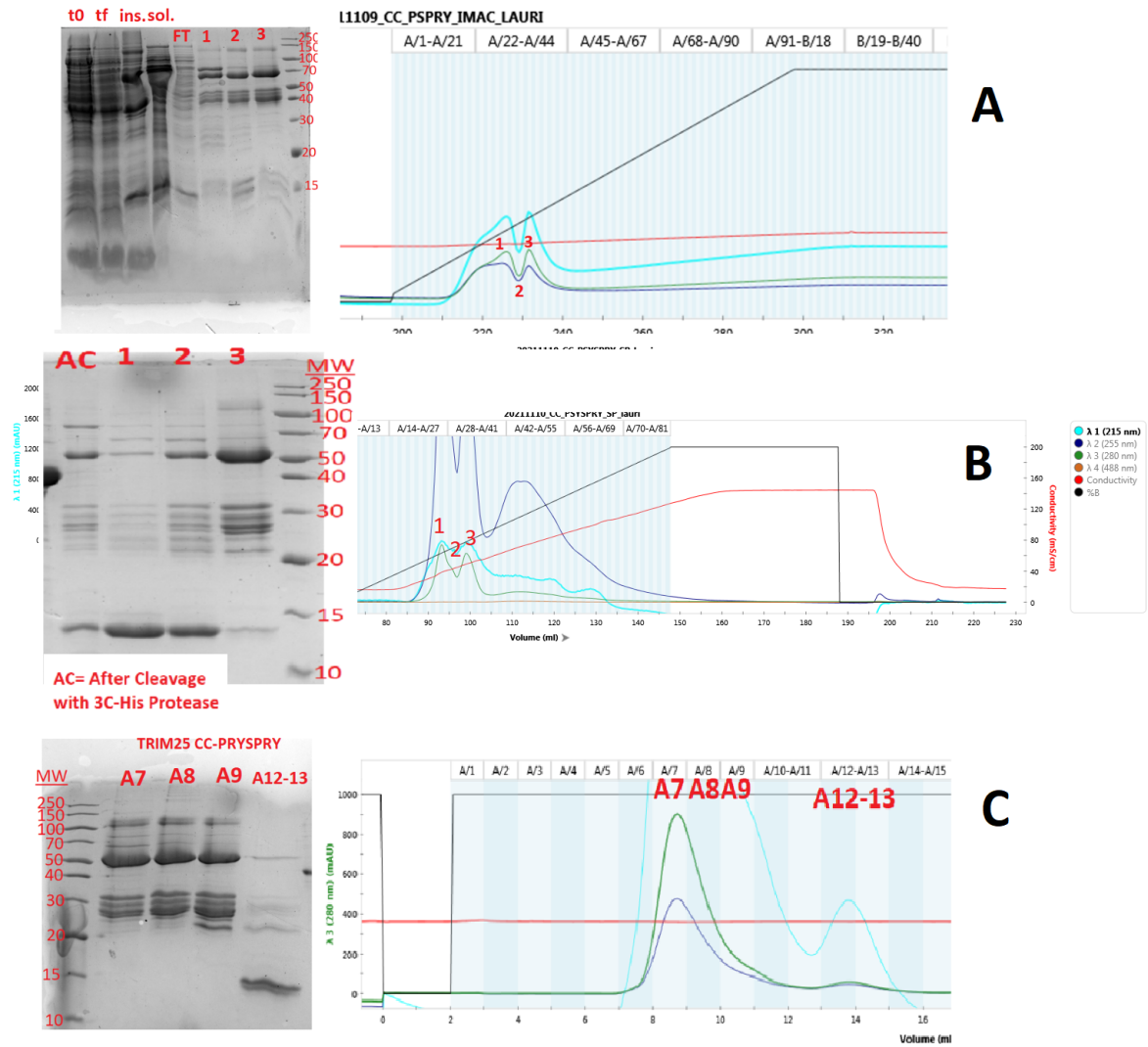
Figure 8 Purification of TRIM25 CC-PRYSPRY domain. Throughout the purification steps, the protein was not homologous on the Coomassie blue-stained SDS-PAGE gel, and the degradation bands are visible. (A) IMAC chromatography (B) Cation Exchange chromatography (C) Size-Exclusion Chromatography.

3.1.2 Expression and Purification of Dicer Hel2i2

We expressed Dicer Hel2i2 in BL21(DE3) strand *E.coli* cells and induced with IPTG when OD reached at 0.6. Cells were lysed by the microfluidizer. Expression of the Dicer Hel2i2 and lysis by microfluidizer were successful (Figure 9).
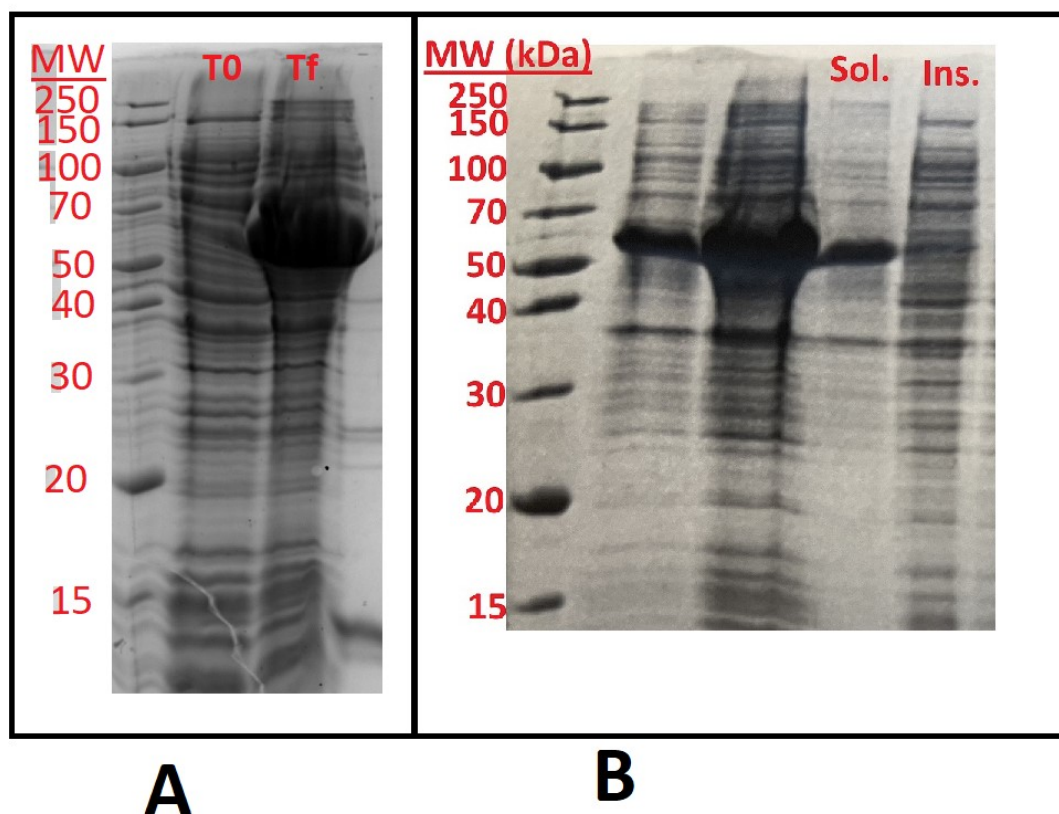
Figure 9 Expression of Dicer Hel2i2 in BL21(DE3) strand E.coli. (A) T0= Cell culture before inducing IPTG, Tf= Cell culture after the induce of IPTG. Expression of Dicer Hel2i2 was successful and produced a bold band in the SDS PAGE gel around 60 kDa. (B) Dicer Hel2i2 protein samples after the lysis by microfluidizer and centrifuging. Sol= Soluble lysate after the centrifuging, which was collected for the IMAC. Ins= Insoluble lysate (pellet) after the centrifuge, no significant amount of the Dicer Hel2i2, which implies that the lysis was successful.

We chose three step purification strategy to determine the purification protocol for Dicer Hel2i2 construct. Immobilized affinity chromatography (IMAC) was used in a first step to capture the protein. Then the protein was cleaved from its His-tag with TEV-protease. Cleaved protein sample was then run again in the IMAC chromatography as intermediate purification step and to remove the HIS-tag from the protein sample. Then the protein was concentrated in a concentrator and size exclusion chromatography was used in last polishing step.

The first purification step, IMAC, produced sharp peak of 3228 mAu (Figure 10).
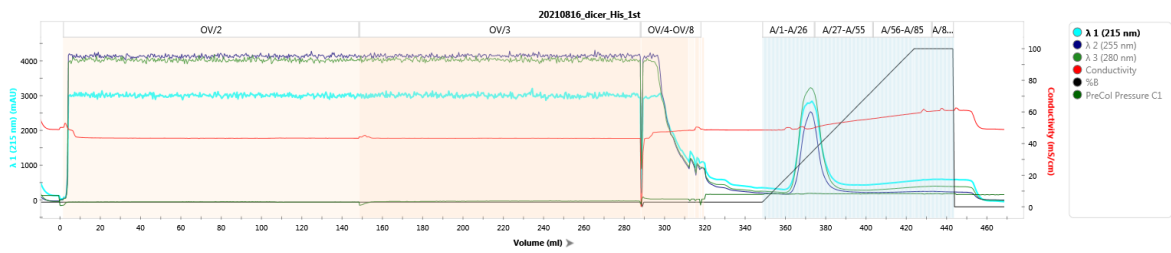
Figure 10 First immobilized affinity column of the Dicer Hel2i2. Sharp peak can be seen around 375 ml.

Protein was cleaved with His-TEV protease and run second time on IMAC column. Cleaved Dicer Hel2i2 does not bind to the column and ends up in the flowthrough. His-Tag binds to the column and is eluted with imidazole. In SDS-PAGE gel (Figure 11) the cleavage was successful by showing two strong bands in the protein sample before the second IMAC (Sample AC). Flowthrough from outlet valves O2 and O3 were collected and in the SDS-PAGE gel there is a strong band of Dicer Hel2i2.
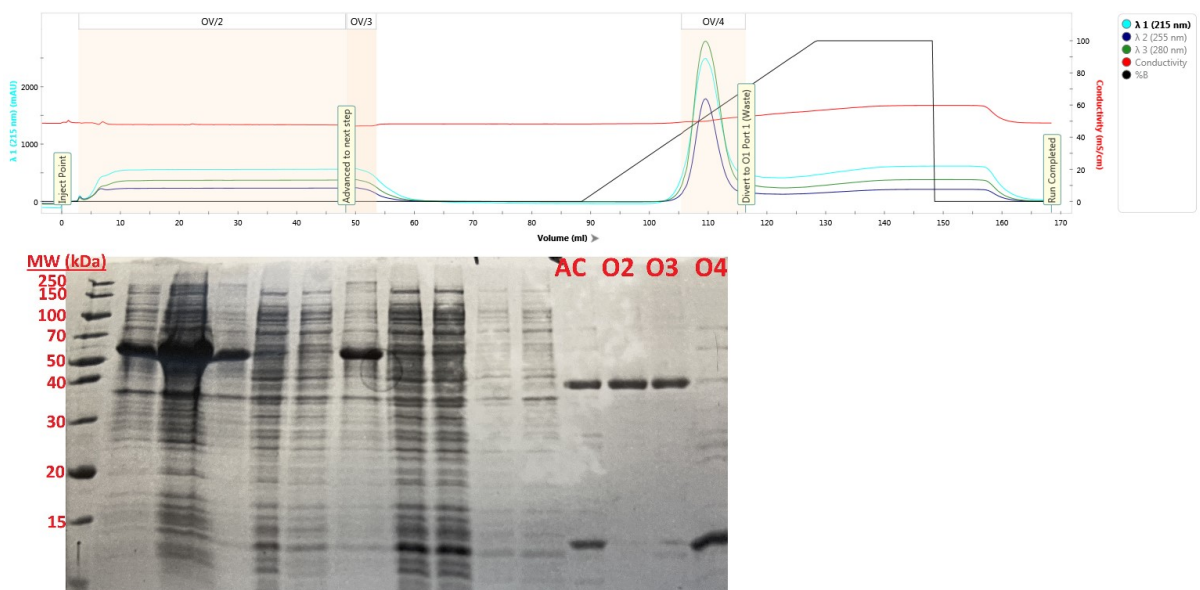

Figure 11 Second nickel affinity column of Dicer Hel2i2 and corresponding SDS-PAGE gel. AC= protein sample after the cleavage with HIS-TEV. There are two visible bands which indicates that the cleavage was successful. Cleaved Dicer Hel2i2 does not bind to IMAC column and is in the flowthrough (Outlet valves OV/2 and OV/2, corresponds to O2 and O3 in the SDS PAGE gel). His-tag binds to the column and gets eluted against the imidazole into the outlet valve 4 (Corresponds to O4 in the gel).

First purification trials with the last purification step, the size exclusive chromatography, were not successful with Dicer Hel2i2. There are no significant peaks in the chromatogram and yield was low (2 mg of protein). When concentrating the protein with Vivaspin® concentrator, the concentration took long time.
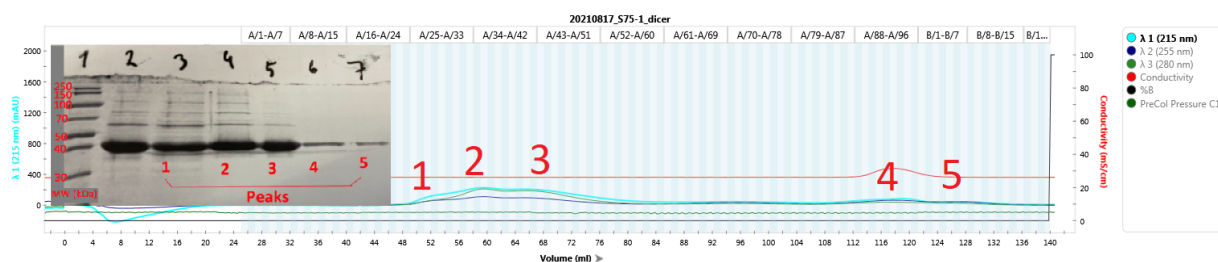

Figure 12 SEC from the first purification trials of Dicer Hel2i2 with corresponding SDS-PAGE gel. There are no clear and sharp peaks visible.

To find optimal buffer conditions for the Dicer Hel2i2, a nanoDsf thermostability screening approach was applied. We carried out NanoDsf experiment with different buffers (Table 1). Figure 13 shows NanoDsf thermograms of Dicer Hel2i2 with different buffer conditions where the relationship between transition from folded state to unfolded state and aggregation of Dicer Hel2i2 can be seen. Figure 13A shows the folding state transition of Dicer Hel2i2 by monitoring the ratio of fluorescence intensity at 330 nm and 350 nm as a function of temperature. Figure 13B shows first derivative of the ratio (intrinsic fluorescence intensity ratio) as a function of temperature. In this result, the optimal buffer for Dicer is 20 mM Sodium Phosphate, pH 6.5, 500 mM NaCl, 2 mM TCEP and 5% glycerol (Figure 13). In this experiment the high concentrated sample number 5 (58.5 µM) denaturated faster in lower temperature than lower concentrated sample number 7 (11.7 µM). This could implicate that the Dicer Hel2i2 is more stable in the lower concentration.

Table 1 NanoDsf experiment with different buffers used (1-13).

|	1	2	3	4	5	6	7	8	9	10	11	12	13
NaH₂PO₄	20 mM	20 mM	20 mM	20 mM	20 mM	20 mM	20 mM	20 mM	20 mM	20 mM	20 mM	20 mM	20 mM
NaCl	500 mM	250 mM	150 mM	150 mM	150 mM	150 mM	150 mM	150 mM	250 mM	500 mM	150 mM	150 mM	150 mM
Glycerol	0%	0%	0%	0%	0%	0%	0%	5%	5%	5%	0%	0%	0%
pH	6.5	6.5	6.5	6.5	6.5	6.5	6.5	6.5	6.5	6.5	7	7.5	8
Dicer Hel 2i2	23.38 µM	23.38 µM	23.38 µM	93.52 µM	58.45 µM	23.38 µM	11.69 µM	23.38 µM	23.38 µM	23.38 µM	23.38 µM	23.38 µM	23.38 µM

Also 0.2 mM TCEP in all samples.
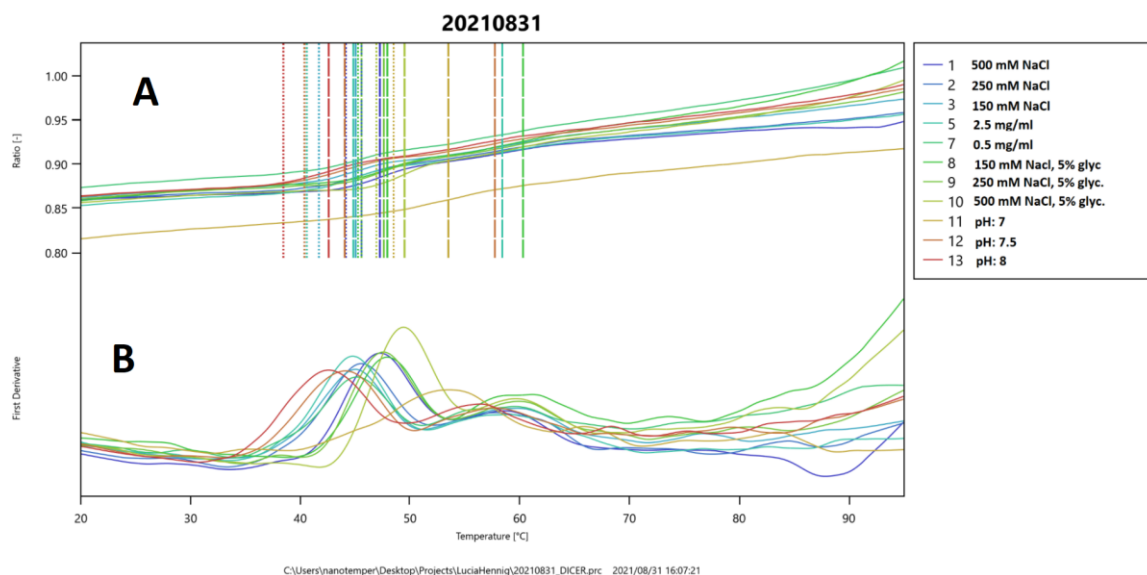
Figure 13 NanoDsf experiment with different buffer conditions. (A) NanoDsf thermogram showing the fluorescence intensity ratio at 330 nm and 350 nm; (B) First derivative of the ratio (intrinsic fluorescence intensity ratio) as a function of temperature.

After testing various buffer conditions with the NanoDsf, we were able to produce Dicer Hel2i2. Especially raising the salt concentration had major impact to the Dicer Hel2i2 yield. A standard purification protocol included a nickel affinity column, TEV cleavage and dialysis, a second nickel affinity column and size exclusion chromatography as a polishing step. To keep Dicer Hel2i2 without aggregating, we avoided high protein concentrations when concentrating the protein.
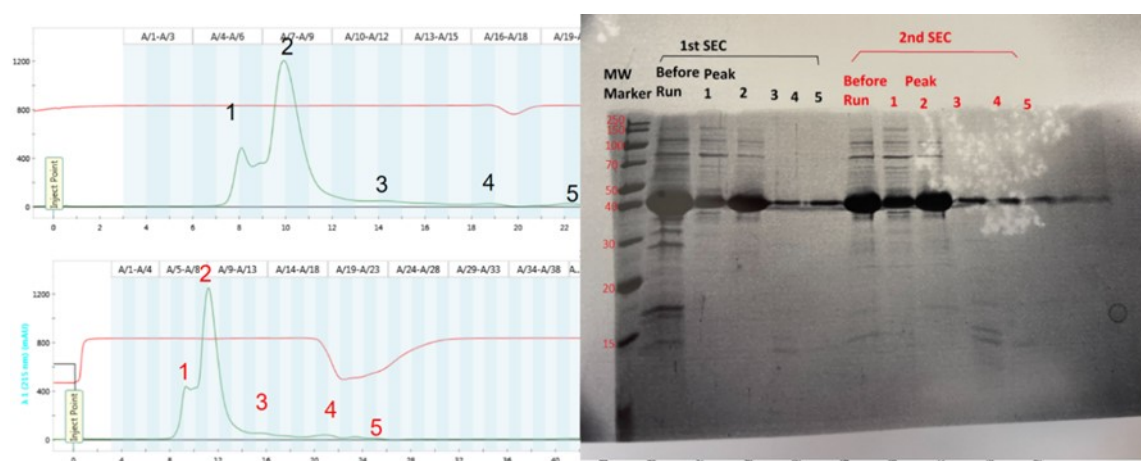

Figure 14 Two runs of SEC of Dicer Hel2i2 with high salt buffer and SDS-PAGE gel corresponding to peaks. Peaks 1 and 3 from both runs were collected. From the SDS-PAGE gel we can still see some impurities from both runs.

3.1.3 Concentration dependance studies of Dicer Hel2i2

To see, if Dicer Hel2i2 aggregates in higher concentrations, we did a concentration dependent study with Dicer Hel2i2. We investigated the oligomeric state of Dicer Hel2i2 domain with NanoDsf, SEC-MALS and NMR.

Table 2 Different concentration dependent studies carried out on Dicer Hel2i2

Experiment	Concentration differences used in a study	Reason for study

NanoDsf	11.7 μM, 23.4 μM and 35.0 μM	Does glycerol have affect on stability to Dicer Hel2i2
SEC-MALS	11.7 μM, 23.4 μM	Is Dicer Hel2i2 monomeric in different concentrations
1-1 Spin Echo 1D NMR	30 μM, 89 μM	Is Dicer Hel2i2 monomeric in NMR spectroscopy

With NanoDsf experiment, we tested out different concentrations of Dicer Hel2i2 with or without glycerol. Tested concentrations were 11.7, 23.4 and 35.0 μM with 3.6, 2.16 and 0.76 % glycerol respectively. Initially we were aiming to have 5 % glycerol in all samples, but due to the calculation error, we had different amount in all samples. There were no significant differences in the results (Figure 15B), but most stable sample were 11.7 μM Dicer Hel2i2 with 3.6 % glycerol. We ran SEC-MALS assay with two different concentrations of Dicer Hel2i2, 23.4 μM and 11.69 μM. Experiments produced peaks near the theoretical weight in both chromatograms. In concentration of 11.69 μM there were also a small additional peak of 88.75 kDa (Figure 15A).
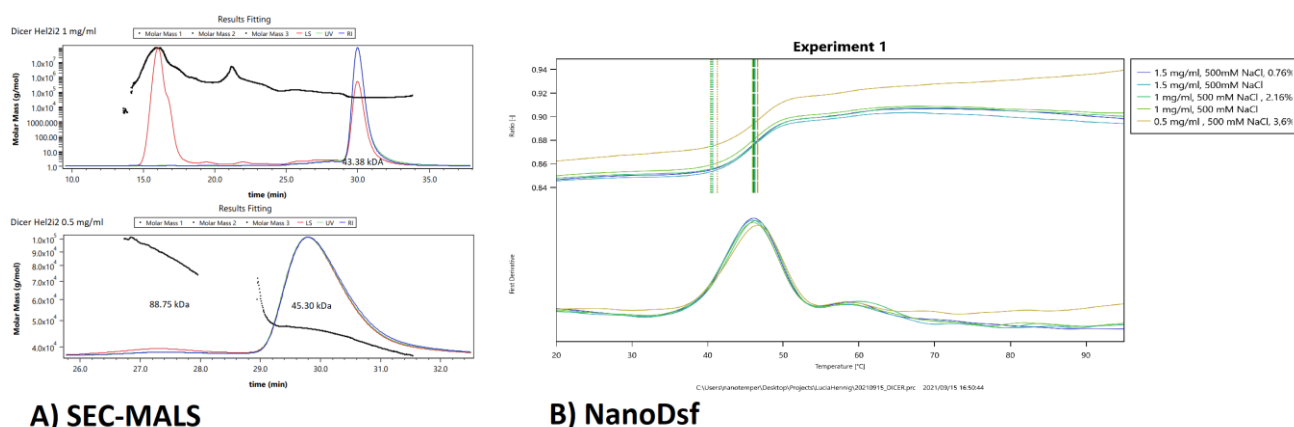
Figure 15 SEC-MALS and NanoDsf experiments regarding the concentration dependance of Dicer Hel2i2. A) SEC-MALS of Dicer HEL2i2 domain with concentration of 23.38 µM and 11.69 µM. Theoretical molecular weight of Dicer Hel2i2 monomer is 42.77 kDa. In both concentrations, there are clear peak near the theoretical molar weight. B) NanoDsf thermogram on different concentrations of Dicer Hel2i2 with or without glycerol. No significant differences between the samples, the most stable sample is 0.5 mg/ml Dicer Hel2i2 with 3.6% glycerol.

For the multimeric state determination with the NMR, we used two different concentrations of Dicer Hel2i2, 89 µM and 30 µM. For concentration of 89 µM, the molecular weight is around 130-180 kDa, depending how we interpret the ratio of I_A/I_B in an overlay spectrum of Dicer and reference spectrum (Figure 16). With lower concentration of Dicer (30 µM), the approximated molecular weight was around 50 kDa. This experiment shows that Dicer oligomerizes in the higher concentration. However, it is good to keep in mind that 1-1 spin echo experiment is not very specific method.
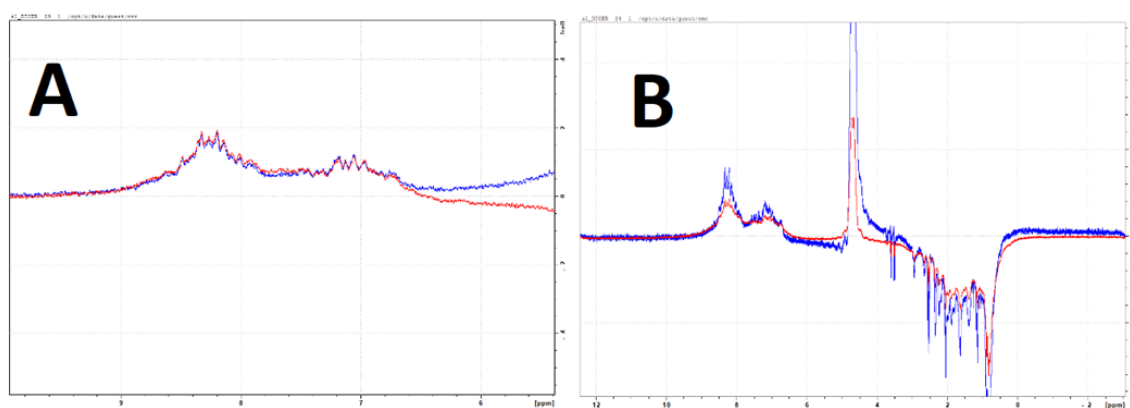
Figure 16 1-1 Echo sequence of Dicer Hel2i2 in different concentrations overlaid to reference spectrum. (A)= Dicer Hel2i2 in concentration of 89 µM. (B) = Dicer Hel2i2 in concentration of 30 µM.

We also tested how the concentration difference effects on HSQC spectra of Dicer Hel2i2. We used two different concentrations of Dicer Hel2i2: 30 µM with 1280 number of scans and 88.6 µM with 256 number of scans. Lower concentration needs more acquisition scans so that the signal to noise ratio is around the same between the samples. With lower concentration, there were more peaks to detect in HSQC spectra (Figure 17). This could imply that Dicer forms aggregates in the 88.6 µM concentration and results to poor HSQC quality spectra.
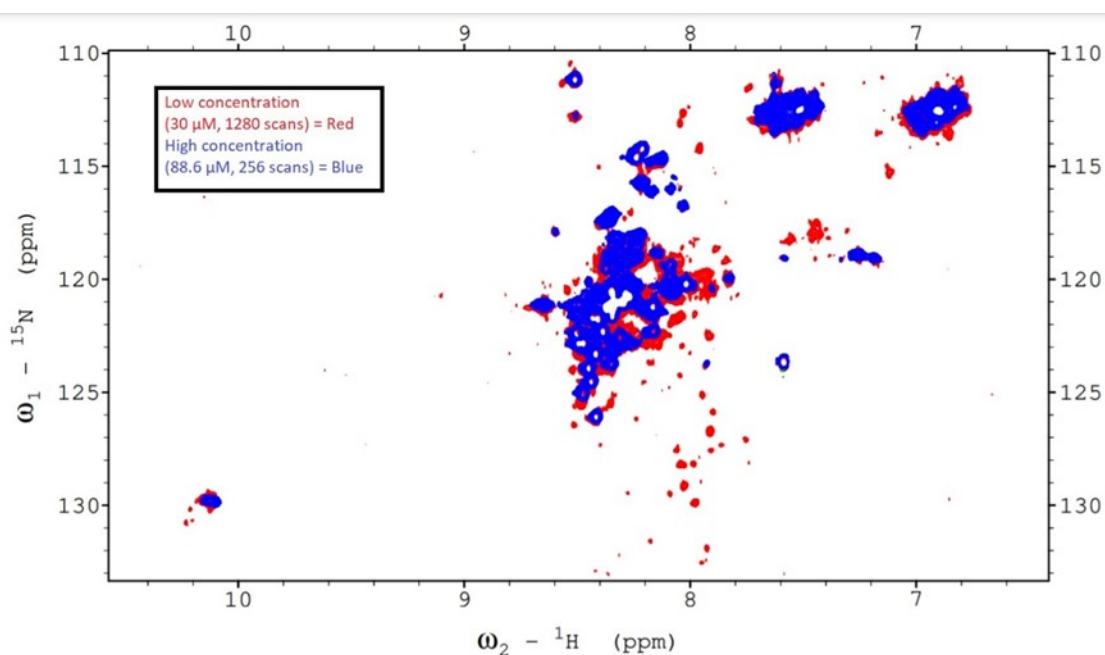
Figure 17 Overlay of Dicer Hel2i2 domains in two different concentrations. We used different amount scans with different concentrations, because in NMR measurements signal to noise ratio increases as the square root of the number of scans. The sample with lower concentration produces more detectable peaks.

3.2 Interaction studies with TRIM25 PRYSPRY and Dicer Hel2i2

For the interaction studies with TRIM25 PRYSPRY and Dicer Hel2i2 we carried out 15N-HSQC NMR titration, SEC-MALS and Mass Photometry assays. NMR chemical shift perturbations (CSPs) indicates the molecular binding. We carried out four different HSQC NMR titrations to see whether there is interaction between Dicer and TRIM25. Titration schemes can be found on table 3. There were no clear evidence for interaction between domains.

Table 3 NMR Titration schemes with TRIM25 PRYSPRY and Dicer Hel2i2

NMR interaction experiment:	Titration steps:	Concentration of labeled sample:
[15N]TRIM25-PRYSPRY + Dicer Hel2i2	1:0.25, 1:0.5, 1:1, 1:1.5, 1:2, 1:3	107 µM
[15N]Dicer Hel2i2 + TRIM25 PRYSPRY	1:0, 1:0.5, 1:1, 1:2, 1:3	88.61 µM
[15N]Dicer Hel2i2 + TRIM25 PRYSPRY	1:0, 1:1, 1:2, 1:3	30 µM

Titration with Dicer Hel2i2 domain and [15N] TRIM25 PRYSPRY domain shows no increase of CSP. However, some of the peaks disappeared (Figure 18). Peaks corresponding to bound state could have disappeared to below the noise level. In the last titration steps, the high concentration of Dicer Hel2i2 might have caused degeneration of sample, resulting to poor quality HSQC spectra.
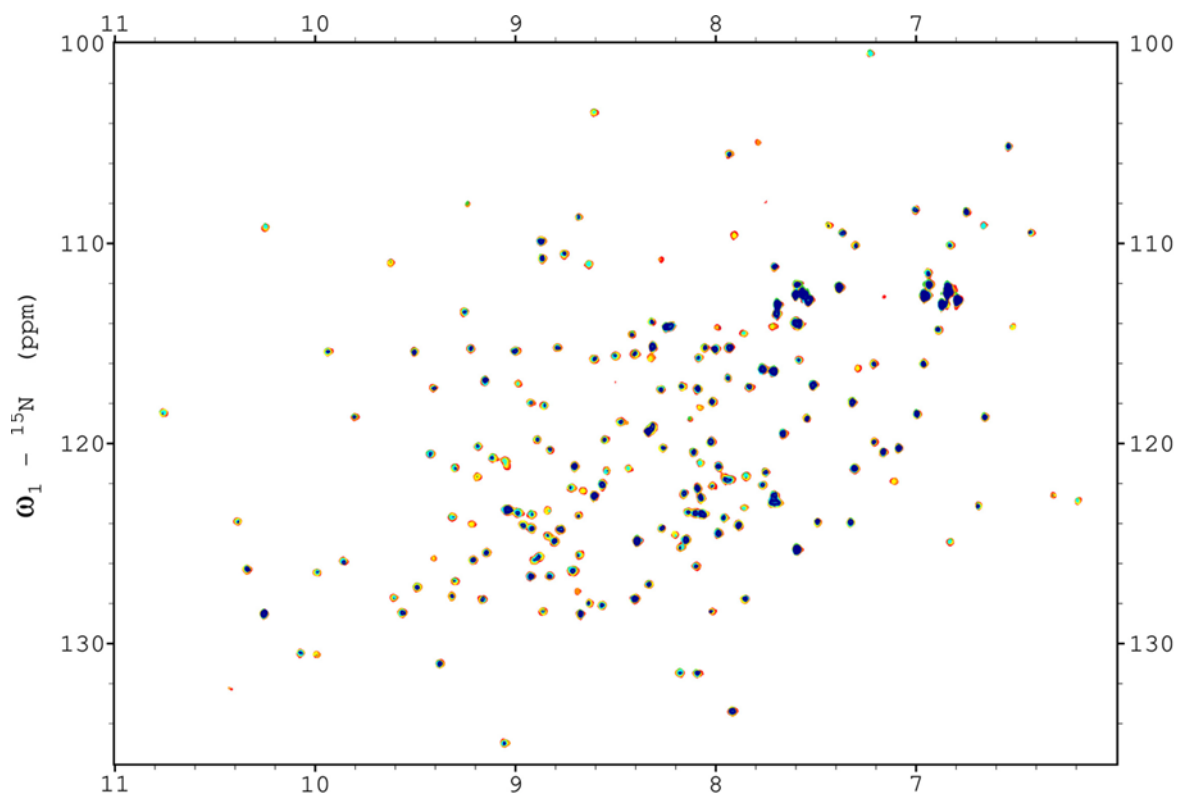
Figure 18 Two-Dimensional HSQC titration of 15N-labeled TRIM25 PRYSPRY and Dicer No clear CSPs. Molar ratios of the ligand to protein concentration are indicated by colours: 0.25; red, 0.5; orange, 1; yellow, 1.5; green, 2; aqua blue, 3; dark blue.

We performed two NMR titration experiments with ^{15}N-labeled Dicer Hel2i2 and TRIM25 PRYSPRY. The experiments varied with the concentration of labeled Dicer Hel2i2 (88.61 µM and 30 µM). No apparent changes in chemical shift dispersion, however a one peak with possible CSP was discovered (Figure 19B), but we cannot verify if it is due to denaturation of sample or interactions between proteins. With lower concentration of Dicer Hel2i2 there are no clear CSPs in the spectrum, but however, there are peaks appearing in area around $\omega 1 = 130$ ppm and $\omega 2 = 8$ ppm (Figure 19A).
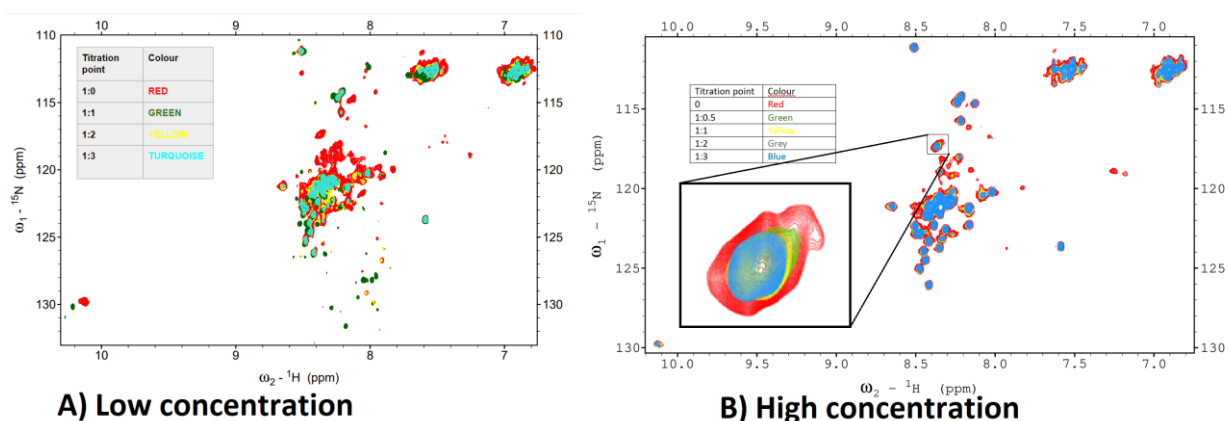
Figure 19 NMR HSQC NMR titrations with 15N labeled Dicer Hel2i2 and TRIM25 PRYSPRY A) Low concentration of Dicer Hel2i2. Molar ratios of the ligand to protein concentration are indicated by colours: 0; red, 0.5; green, 1; green, 2; yellow, 3; turquoise. B) High concentration of Dicer Hel2i2. Molar ratios of the ligand to protein concentration are indicated by colours: 0; red, 0.5; green, 1; yellow, 2; grey, 3; blue.

SEC-MALS experiment with TRIM25 PRYSPRY and Dicer Hel2i2 shows three peaks: 24.4 kDa, 45.7 kDa and 114.3 kDa (Figure 20). The small peak of 114.3 kDa could possibly be a complex which is formed by the dimer of the peak 45.7 kDa and the monomer of peak 24.4 kDa (combined mass 115.8 kDa). TRIM25 PRYSPRY monomer could be assigned to peak of 24.4 kDa, which is slightly bigger than the theoretical mass of PRYSPRY (22.0 kDa), but within the error range. Dicer Hel2i2 could be the peak corresponding to molecular weight of 45.7 kDa (theoretical mass of Dicer Hel2i2 42.8 kDa).
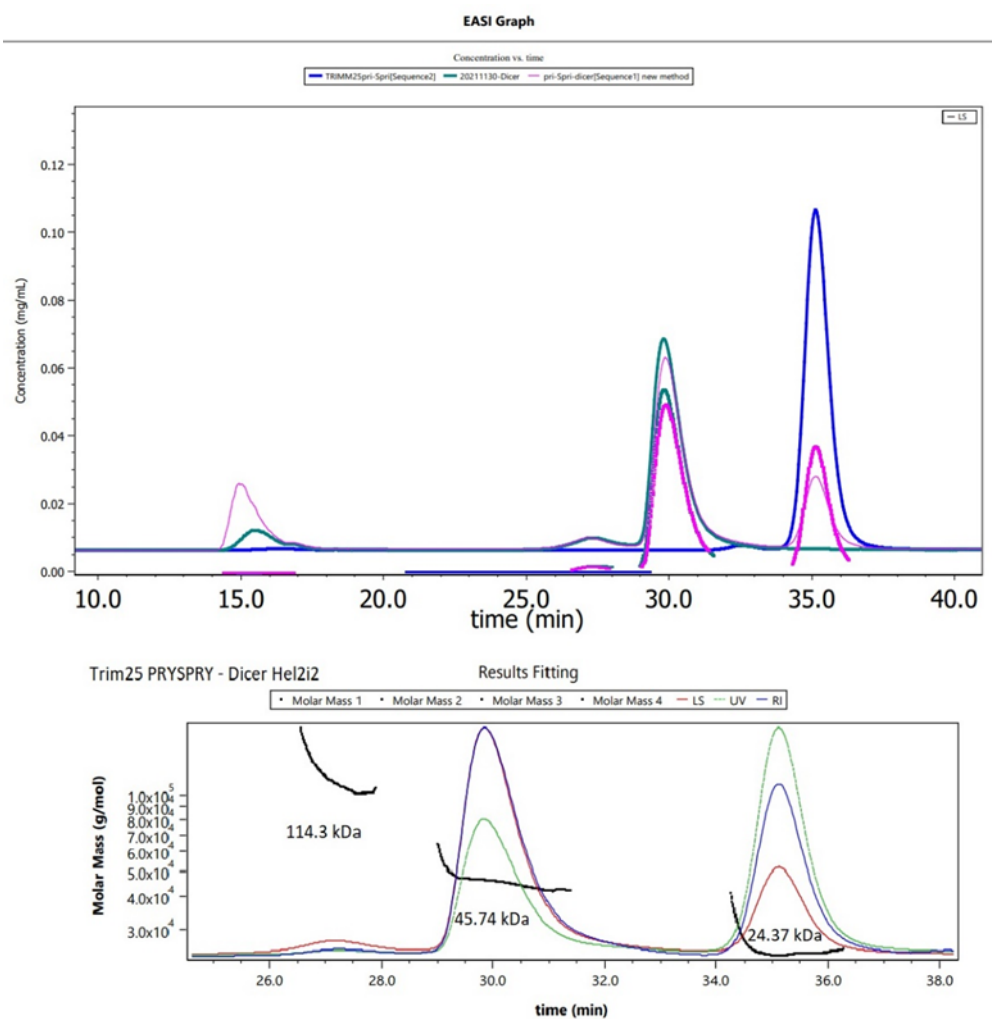
Figure 20 SEC-MALS overlay. Dicer Hel2i2 and TRIM25 PRYSPRY forms three peaks (24.37, 45.74 and 114.3 kDa). 24.37 kDa peak is believed to be PRYSPRY monomer, 45.74 kDa Dicer Hel2i2 monomer and 114.3 kDa could be aggregates or dimerized Dicer and PRYSPRY domain.

Mass photometry assays between Dicer Hel2i2 and TRIM25 PRYSPRY shows that most of the counts corresponds to molecular weight of 47 kDa, which could imply to Dicer Hel2i2 monomer within the margin of error (Figure 21).
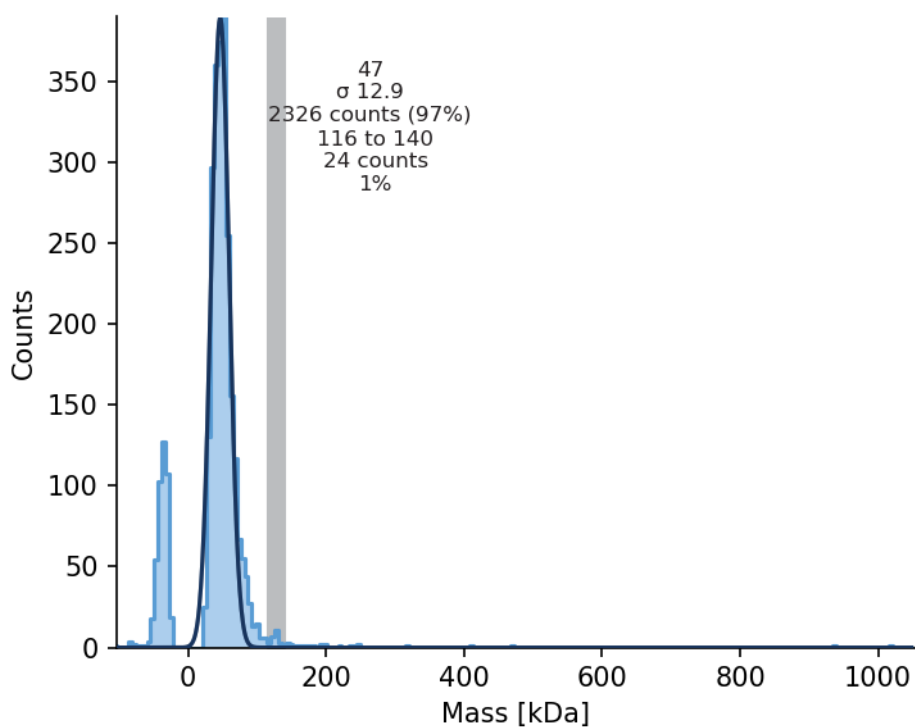
Figure 21 Histogram of solution of Dicer Hel2i2 and TRIM25 PRYSPRY. 97 percent of counts corresponds to molecular weight of 47 kDa which could imply to Dicer Hel2i2 monomer (42.77 kDa). Monomer of Trim25 PRYSPRY not visible due to restrictions of the mass photometry.

3.3 INTERACTION STUDIES WITH TRIM25 CC-PRYSPRY AND DICER HEL2I2

For the interaction studies with TRIM25 CC-PRYSPRY and Dicer Hel2i2, we carried out an NMR HSQC titration, SEC-MALS and mass photometry. NMR titration scheme can be found on table 4. No clear evidence for the interaction between domains were found.

Table 4 NMR titration scheme with 15N TRIM25 CC-PRYSPRY and Dicer Hel2i2

NMR HSQC titration	Titration steps	Concentration of labeled sample
[15N]TRIM25 CC-PRYSPRY + Dicer Hel2i2	1:0, 1:0.25, 1:0.5, 1:0.8	27 µM

The NMR HSQC titration with Dicer Hel2i2 and TRIM25 CC-PRYSPRY domain shows no apparent changes in chemical shift dispersion in the spectrum (Figure 22). Signal dispersion of spectrums are poor, which is characteristic for unfolded proteins and needs to be taken into consideration when interpreting results.
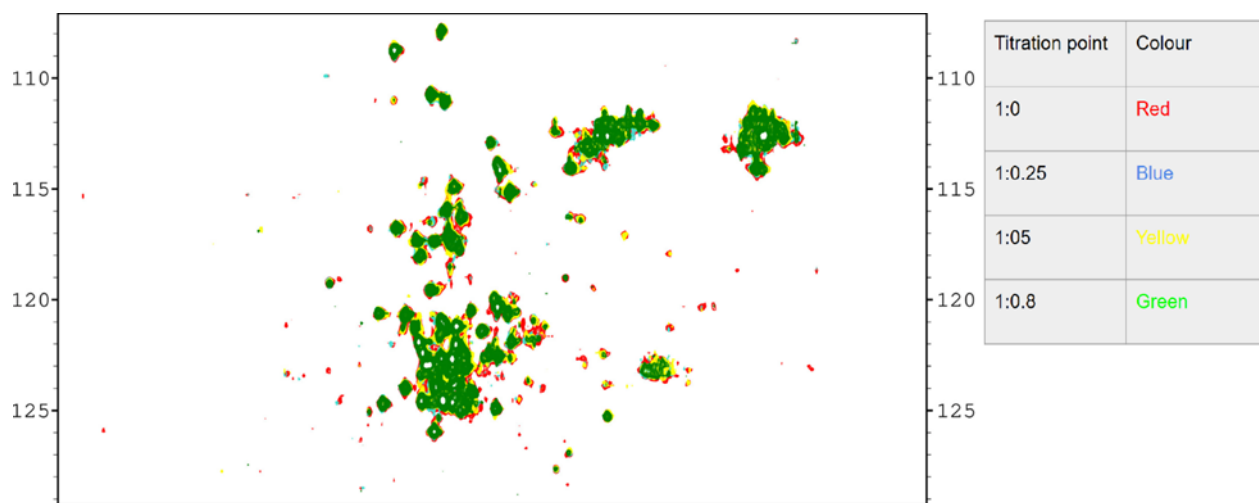

Figure 22 TRIM25 CC-PRYSRPRY NMR titration with Dicer. Molar ratios of the ligand to protein concentration are indicated by colours: 0; red, 0.25; blue, 0.5; yellow, 0.8; green.

The SEC-MALS assay with TRIM25 CC-PRYSPRY and Dicer Hel2i2 shows four peaks corresponding to molecular weights of 47.6, 63.1, 80.84 and 137 kDa (Figure

23). The peak 47.6 kDa could consist of both TRIM25 CC-PRYSPRY and Dicer Hel2i2 domains. We detected two peaks with molecular weight of 63.1 and 80.84 kDa that we had difficulties to assign. The peak 137 kDa could potentially be a complex consisting of the CC-PRYSPRY and Hel2i2 domains or aggregates and impurities due to poor purity of the sample.
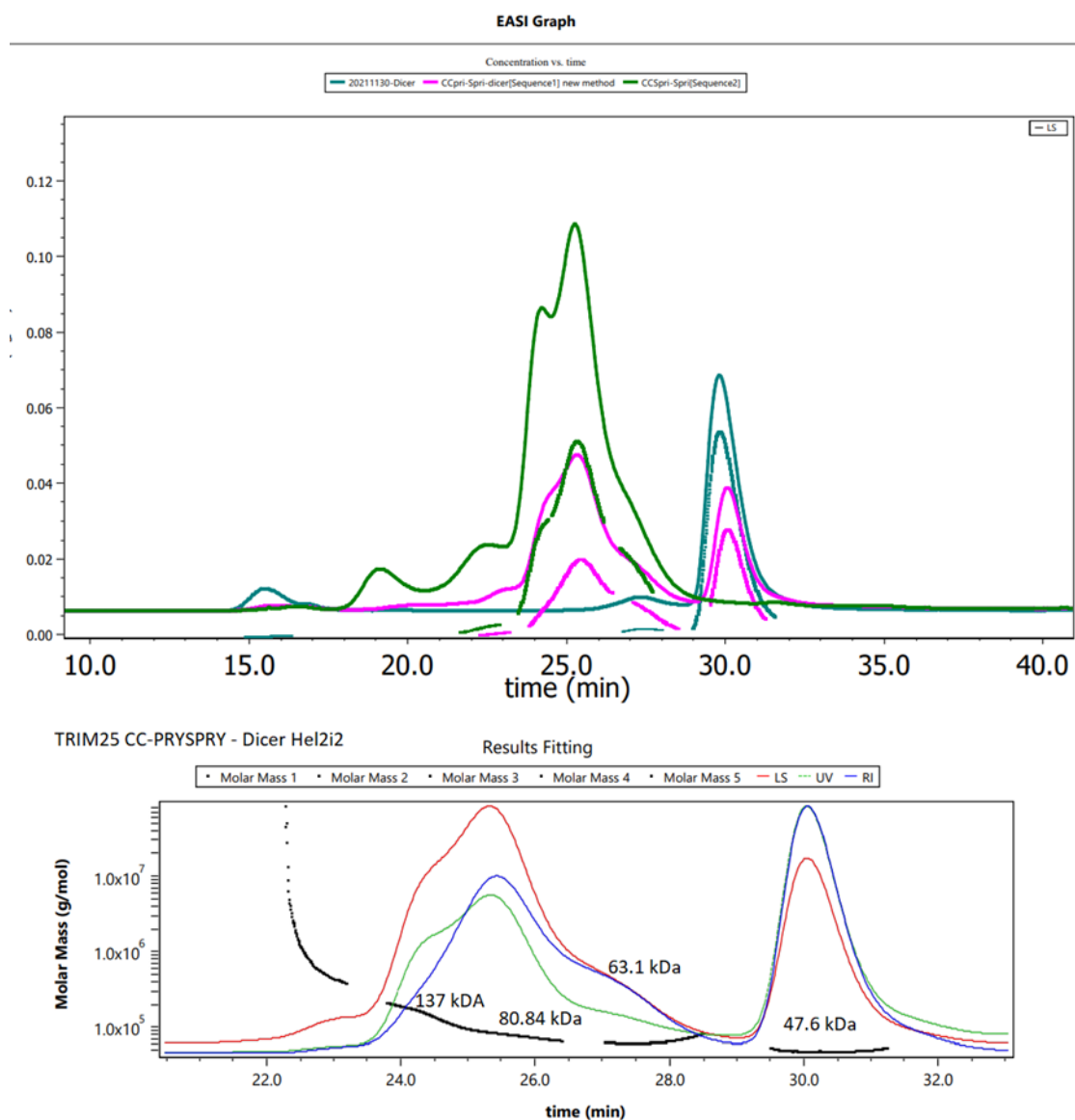

Figure 23 SEC-MALS with TRIM25 CC-PRYSPRY and Dicer Hel2i2 shows four peaks (47.6, 63.1, 80.8 and 137.0 kDa). Peak of 47.6 kDa could be composed of both proteins. Peaks 63.1 and 80.8 kDa are hard to assign and could be impurities of the sample. Peak 137 kDa

can be a complex of proteins from the peak of 47.6 kDa or aggregates and impurities of the sample.

Mass photometry with Dicer Hel2i2 and TRIM25 CC-PRYSPRY shows two distinct peaks in the molecular weight of 51 and 70 kDa (Figure 24). 12 Percent of the counts are in the molecular weight of 102 kDa. One percent of the counts are in the molecular weight of 146 kDa, which is near the theoretical weight of CC-PRYSPRY dimer and Dicer Hel2i2 monomer complex.

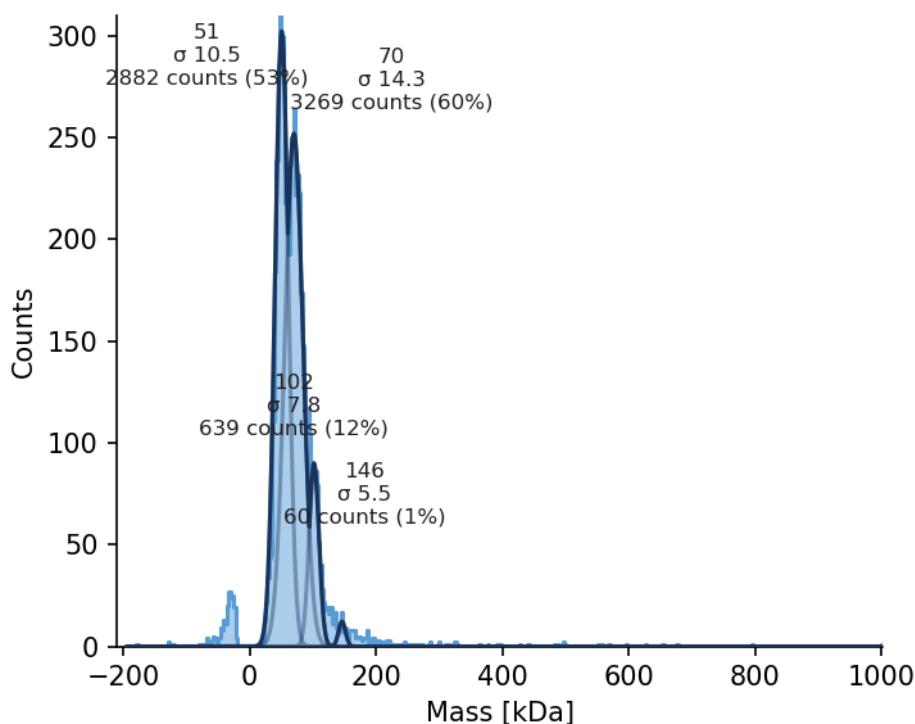*Figure 24 Histogram of solution of Dicer Hel2i2 and TRIM25 CC-PRYSPRY. There are high peak in 51 kDa (53 % of counts) which could be Dicer Hel2i2 monomer. Also, a peak in molecular weight of 102 which could be TRIM25 CC-PRYSPRY dimer. 60 count (1%) peak forms into the molecular weight of 146 kDa, which could be TRIM25 CC-PRYSPRY dimer and Dicer Hel2i2. Unknown peak in the 70 kDa with 60 % of counts.*

4 CONCLUSIONS AND DISCUSSION

4.1 EXPRESSION AND PURIFICATION OF THE PROTEINS

We managed to succeed our secondary aim of the study to set a working purification protocol for the Dicer Hel2i2 domain. From the SDS-PAGE gel we could still see some impurities after the size-exclusion chromatography. Despite that, Dicer Hel2i2 was still pure enough to use in further studies. The problem we faced with the concentration dependance studies was that we could not have the same concentration in all studies (NanoDsf, SEC-MALS, NMR), because of the yield of Dicer Hel2i2 varied on different batches we produced. However, our research shows that Dicer Hel2i2 tends to form aggregates in higher concentrations. According to our data from NanoDsf and SEC-MALS experiments, Dicer Hel2i2 is a monomer in concentration of 30 µM with salt concentration of 500 mM and 5% glycerol. Protein aggregation is closely related to the thermal stability of proteins, so the Dicer Hel2i2 should always keep on ice when working with it. Our yield of the protein was also quite low. From 6 liters of bacterial media, we were able to get approximately 10 mg of Dicer Hel2i2. In the future, I believe the yield can be increased by improving the process steps and by gaining more experience working with Dicer Hel2i2 domain.

The expression and purification of TRIM25 PRYSPRY was successful, and the final product was concentrated and pure enough to use in further studies. With the TRIM25 CC-PRYSPRY, we were not so successful. There were degenerated bands throughout the purification process on a SDS-PAGE gel. We were not able to track

down the reason why the purification was not successful. To avoid degradation by proteases during the purification, we used protease inhibitory cocktail. We also kept the protein sample on ice between the purification steps. In our lab, we have produced TRIM25 CC-PRYSPRY before and the protocol has worked so far. We speculate that the plasmid we used were defective. Unfortunately due to limited working time on a lab, we did not have time to verify the integrity of the plasmid or order a new one.

4.2 BINDING EXPERIMENTS

Regardless our difficulties to produce pure and concentrated proteins, we were able to use TRIM25 CC-PRYSPRY, TRIM25 PRYSPRY and Dicer Hel2i2 domains to characterize the interaction between TRIM25 and Dicer. Overall, we did not detect any markable interactions. With Dicer Hel2i2 and TRIM25 PRYSPRY this was in line with our hypothesis because we predicted that TRIM25 PRYSPRY does not interact with Dicer Hel2i2 due to its monomer composition.

Lack of interactions between TRIM25 CC-PRYSPRY and Dicer Hel2i2 may have been due to issues producing stable TRIM25 CC-PRYSPRY and Dicer Hel2i2, but also these proteins are relatively big for the NMR spectroscopy and high salt concentration of Dicer Hel2i2 sets challenges for NMR studies. High temperature of NMR spectrometer (25°C) and long acquisition times also affects to proteins viability. Furthermore, the interaction between the proteins might be very transient and weak and no stable complex is not formed in the salt and buffer conditions used.

One thing to take into consideration is the RNA dependency to TRIM25 activity. RNA binding might increase TRIM25 activity through allosteric changes or RNA could facilitate the interaction when substrates bind to the same RNA. For example, there is no clear evidence of direct interaction between TRIM25 and RIG-I *in vitro*,

which could suggest that RNA is needed for the interaction (Williams et al. 2019). RNA could also stabilize the CC-PRYSPRY or allosterically modulate the domain structure. In further studies, it would be interesting to characterizing the interaction between DICER and TRIM25 with presence of RNA.

4.3 CONCLUDING REMARKS

Molecular mechanisms and the interaction between TRIM25 and Dicer on a residue level is still lacking despite the importance of antiviral properties of both proteins. Understanding the virus-host interactions and innate immunity mechanism is important for developing effective therapies to prevent the future viral outbreaks. In this study I provided more insights what to take to consideration when planning for interaction studies for Dicer and TRIM25. Improving the purification and sample preparation steps and conditions would produce better and more reliable results.

Both proteins are shown to be important actors in immune defense and attractive targets for therapeutic use. In the future more characteristic studies related to human Dicer Hel2i2 and TRIM25 are required and in what biological context these interactions occur. Especially the crystal structure of a Dicers Helicase domain would help future scientists to resolve the questions related to our immune defense against viral pathogens. One key question is also to find out how Dicer acquire Ub-dependent and Ub-independent regulatory functions of TRIM25.

ACKNOWLEDGES

LITERATURE

Ahmad, S. & Hur, S. 2015. Helicases in Antiviral Immunity: Dual Properties as Sensors and Effectors. Trends in biochemical sciences (Amsterdam. Regular ed.), 40(10), pp. 576-585. doi:10.1016/j.tibs.2015.08.001

Akutsu, M., Dikic, I. & Bremm, A. 2016. Ubiquitin chain diversity at a glance. Journal of cell science, 129(5), pp. 875-880. doi:10.1242/jcs.183954

Anglister, J., Grzesiek, S., Ren, H., Klee, C. B. & Bax, A. 1993. Isotope-edited multidimensional NMR of calcineurin B in the presence of the non-deuterated detergent CHAPS. Journal of biomolecular NMR, 3(1), pp. 121-126. doi:10.1007/BF00242480

Buchmann, K. 2014. Evolution of Innate Immunity: Clues from Invertebrates via Fish to Mammals. Frontiers in immunology, 5, p. 459. doi:10.3389/fimmu.2014.00459

Choudhury, N. R., Heikel, G., Trubitsyna, M., Kubik, P., Nowak, J. S., Webb, S., . . . Michlewski, G. 2017. RNA-binding activity of TRIM25 is mediated by its PRY/SPRY domain and is required for ubiquitination. BMC biology, 15(1), p. 105. doi:10.1186/s12915-017-0444-9

Ciechanowska, K., Pokornowska, M. & Kurzyńska-Kokorniak, A. 2021. Genetic Insight into the Domain Structure and Functions of Dicer-Type Ribonucleases. International journal of molecular sciences, 22(2), p. 616. doi:10.3390/ijms22020616

D'Cruz, A. A., Kershaw, N. J., Chiang, J. J., Wang, M. K., Nicola, N. A., Babon, J. J., . . . Nicholson, S. E. 2013. Crystal structure of the TRIM25 B30.2 (PRYSPRY) domain: A key component of antiviral signalling. Biochemical journal, 456(2), pp. 231-240. doi:10.1042/BJ20121425

Delaglio F, Grzesiek S, Vuister GW, Zhu G, Pfeifer J, Bax A. NMRPipe: a multidimensional spectral processing system based on UNIX pipes. J Biomol NMR. 1995 Nov;6(3):277-93. doi: 10.1007/BF00197809. PMID: 8520220.

Doyle, M., Badertscher, L., Jaskiewicz, L., Güttinger, S., Jurado, S., Hugenschmidt, T., . . . Filipowicz, W. 2013. The double-stranded RNA binding domain of human Dicer functions as a nuclear localization signal. RNA (Cambridge), 19(9), pp. 1238-1252. doi:10.1261/rna.039255.113

Fairman-Williams, M. E., Guenther, U. & Jankowsky, E. 2010. SF1 and SF2 helicases: Family matters. Current opinion in structural biology, 20(3), pp. 313-324. doi:10.1016/j.sbi.2010.03.011

Hansen, S. R., Aderounmu, A. M., Donelick, H. M. & Bass, B. L. 2019. Dicer's Helicase Domain: A Meeting Place for Regulatory Proteins. Cold Spring Harbor Symposia on Quantitative Biology, 84, pp. 185-193. doi:10.1101/sqb.2019.84.039750

Haubrich, K., Augsten, S., Simon, B., Masiewicz, P., Perez, K., Lethier, M., Rittinger, K., Gabel, F., Cusack, S. & Hennig, J. 2020. RNA binding regulates TRIM25-mediated RIG-I ubiquitylation. bioRxiv 2020.05.04.070177; doi: https://doi.org/10.1101/2020.05.04.070177

Heikel, G., Choudhury, N. R. & Michlewski, G. 2016. The role of Trim25 in development, disease and RNA metabolism. Biochemical Society transactions, 44(4), p. 1045.

Jankowsky, E. & Fairman, M. E. 2007. RNA helicases — one fold for many functions. Current opinion in structural biology, 17(3), pp. 316-324. doi:10.1016/j.sbi.2007.05.007

Kato, K., Ahmad, S., Zhu, Z., Young, J. M., Mu, X., Park, S., . . . Hur, S. 2021. Structural analysis of RIG-I-like receptors reveals ancient rules of engagement between diverse RNA helicases and TRIM ubiquitin ligases. Molecular cell, 81(3), pp. 599-613.e8. doi:10.1016/j.molcel.2020.11.

Kim, S. H., Yoo, H. J., Park, E. J. & Na, D. H. 2021. Nano Differential Scanning Fluorimetry-Based Thermal Stability Screening and Optimal Buffer Selection for Immunoglobulin G. Pharmaceuticals (Basel, Switzerland), 15(1), p. 29. doi:10.3390/ph15010029

Kowalinski, E. 2010. Structural studies of host-virus interactions looking at two examples: the innate immunity receptor RIG-I and the influenza virus RNA polymerase endonuclease. Biochemistry, Molecular Biology. Université Joseph-Fourier - Grenoble I. English. fftel-00752678f

Korhonen, H. M., Meikar, O., Yadav, R. P., Papaioannou, M. D., Romero, Y., Da Ros, M., . . . Kotaja, N. 2011. Dicer Is Required for Haploid Male Germ Cell Differentiation in Mice. PloS one, 6(9), p. e24821. doi:10.1371/journal.pone.0024821

Kurzynska-Kokorniak, A., Koralewska, N., Pokornowska, M., Urbanowicz, A., Tworak, A., Mickiewicz, A. & Figlerowicz, M. 2015. The many faces of Dicer: The complexity of the mechanisms regulating Dicer gene expression and

enzyme activities. Nucleic acids research, 43(9), pp. 4365-4380. doi:10.1093/nar/gkv328 5.

Leitão, A. L., Costa, M. C. & Enguita, F. J. 2015. Unzippers, resolvers and sensors: A structural and functional biochemistry tale of RNA helicases. International journal of molecular sciences, 16(2), pp. 2269-2293. doi:10.3390/ijms16022269

Li, Y., Lu, J., Han, Y., Fan, X. & Ding, S. 2013. RNA Interference Functions as an Antiviral Immunity Mechanism in Mammals. Science (American Association for the Advancement of Science), 342(6155), pp. 231-234. doi:10.1126/science.1241911

Li, Y., Struwe, W. B. & Kukura, P. 2020. Single molecule mass photometry of nucleic acids. Nucleic acids research, 48(17), p. e97. doi:10.1093/nar/gkaa632

Linder, P. & Jankowsky, E. 2011. From unwinding to clamping — the DEAD box RNA helicase family. Nature reviews. Molecular cell biology, 12(8), pp. 505-516. doi:10.1038/nrm3154

Liu, Z., Wang, J., Cheng, H., Ke, X., Sun, L., Zhang, Q. C. & Wang, H. 2018. Cryo-EM Structure of Human Dicer and Its Complexes with a Pre-miRNA Substrate. Cell, 173(6), pp. 1549-1550. doi:10.1016/j.cell.2018.05.031

Luo, D., Kohlway, A. & Pyle, A. M. 2013. Duplex RNA activated ATPases (DRAs): Platforms for RNA sensing, signaling and processing. RNA biology, 10(1), pp. 111-120. doi:10.4161/rna.22706

Ma, E., MacRae, I. J., Kirsch, J. F. & Doudna, J. A. 2008. Autoinhibition of Human Dicer by Its Internal Helicase Domain. Journal of molecular biology, 380(1), pp. 237-243. doi:10.1016/j.jmb.2008.05.005

Maillard, P. V., Veen, A. G., Poirier, E. Z. & Reis e Sousa, C. 2019. Slicing and dicing viruses: Antiviral RNA interference in mammals. The EMBO journal, 38(8), pp. -n/a. doi:10.15252/embj.2018100941

de Marco, A. 2007. Protocol for preparing proteins with improved solubility by co-expressing with molecular chaperones in Escherichia coli. Nature protocols, 2(10), pp. 2632-2639. doi:10.1038/nprot.2007.400

Nguyen, N. T. H., Now, H., Kim, W., Kim, N. & Yoo, J. 2016. Ubiquitin-like modifier FAT10 attenuates RIG-I mediated antiviral signaling by segregating activated RIG-I from its signaling platform. Scientific reports, 6(1), p. 23377. doi:10.1038/srep23377

Paturi, S. & Deshmukh, M. V. 2021. A Glimpse of "Dicer Biology" Through the Structural and Functional Perspective. Frontiers in molecular biosciences, 8, p. 643657. doi:10.3389/fmolb.2021.643657

Sanchez, J. G., Sparrer, K. M., Chiang, C., Reis, R. A., Chiang, J. J., Zurenski, M. A., . . . Pornillos, O. 2018. TRIM25 Binds RNA to Modulate Cellular Anti-viral Defense. Journal of molecular biology, 430(24), pp. 5280-5293. doi:10.1016/j.jmb.2018.10.003

Schuster, S., Miesen, P. & Rij, R. v. 2019. Antiviral RNAi in Insects and Mammals: Parallels and Differences. Viruses, 11(5), p. 448. doi:10.3390/v11050448

Shaid, S., Brandts, C. H., Serve, H. & Dikic, I. 2013. Ubiquitination and selective autophagy. Cell death and differentiation, 20(1), pp. 21-30. doi:10.1038/cdd.2012.72

Sklenář, V., Brooks, B. R., Zon, G. & Bax, A. 1987. Absorption mode two-dimensional NOE spectroscopy of exchangeable protons in oligonucleotides. FEBS letters, 216(2), pp. 249-252. doi:10.1016/0014-5793(87)80699-3

Song, M. & Rossi, J. J. 2017. Molecular mechanisms of Dicer: Endonuclease and enzymatic activity. Biochemical journal, 474(10), pp. 1603-1618. doi:10.1042/BCJ20160759

Svobodova, E., Kubikova, J. & Svoboda, P. 2016. Production of small RNAs by mammalian Dicer. Pflügers Archiv, 468(6), pp. 1089-1102. doi:10.1007/s00424-016-1817-6

Vaishali, V., Dimitrova-Paternoga, L., Haubrich, K., Sun, M., Ephrussi, A. & Hennig, J. 2021. Validation and classification of RNA binding proteins identified by mRNA interactome capture. bioRxiv. doi:10.1101/2021.02.02.429302

Vincenzi, B., Iuliani, M., Zoccoli, A., Pantano, F., Fioramonti, M., De Lisi, D., . . . Tonini, G. 2015. Deregulation of dicer and mir-155 expression in liposarcoma. Oncotarget, 6(12), pp. 10586-10591. doi:10.18632/oncotarget.3201

Wen, J., Lord, H., Knutson, N. & Wikström, M. 2020. Nano differential scanning fluorimetry for comparability studies of therapeutic proteins. Analytical biochemistry, 593, p. 113581. doi:10.1016/j.ab.2020.113581

Williams, F. P., Haubrich, K., Perez-Borrajero, C. & Hennig, J. 2019. Emerging RNA-binding roles in the TRIM family of ubiquitin ligases. Biological chemistry, 400(11), p. 1443.

Wojnicka, M., Szczepanska, A. & Kurzynska-Kokorniak, A. 2020. Unknown Areas of Activity of Human Ribonuclease Dicer: A Putative Deoxyribonuclease Activity. Molecules (Basel, Switzerland), 25(6), p. 1414. doi:10.3390/molecules25061414

Zamore, P. D. & Ghildiyal, M. 2009. Small silencing RNAs: An expanding universe. Nature reviews. Genetics, 10(2), pp. 94-108. doi:10.1038/nrg2504

Zheng, X., Wang, X., Tu, F., Wang, Q., Fan, Z. & Gao, G. 2017. TRIM25 Is Required for the Antiviral Activity of Zinc Finger Antiviral Protein. Journal of virology, 91(9), . doi:10.1128/JVI.00088-17